Palaeogeography, Palaeoclimatology, Palaeoecology xxx (2014) xxx–xxx

Contents lists available at ScienceDirect

Palaeogeography, Palaeoclimatology, Palaeoecology

journal homepage: www.elsevier.com/locate/palaeo

Foraminiferal and nannofossil paleoecology and paleoceanography of the Cenomanian–Turonian Eagle Ford Shale of southern Texas

Christopher M. Lowery [a,*], Matthew J. Corbett [b], R. Mark Leckie [a], David Watkins [b], Andrea Miceli Romero [c], Aris Pramudito [d]

[a] Univeristy of Massachusetts, Dept. of Geosciences, 233 Morrill Science Center, 611 N. Pleasant St., Amherst, MA 01003, USA
[b] University of Nebraska, Dept. of Earth and Atmospheric Sciences, 214 Bessey Hall, PO Box 80330, Lincoln, NE 68588, USA
[c] University of Oklahoma, School of Geology and Geophysics, 100 East Boyd St., Room 710, Norman, OK 73019, USA
[d] BP, 501 Westlake Park Blvd., Houston, TX 77079, USA

ARTICLE INFO

Article history:
Received 3 July 2013
Received in revised form 21 July 2014
Accepted 23 July 2014
Available online xxxx

Keywords:
OAE2
Foraminiferal paleoecology
Calcareous nannofossil paleoecology
Eagle Ford Shale
Western Interior Seaway

ABSTRACT

The Upper Cretaceous of central Texas is dominated by a broad, shallow carbonate platform called the Comanche Platform that occupies an important gateway between the epeiric Western Interior Seaway (WIS) of North America to the open-marine Gulf of Mexico/Tethys. We investigated the Cenomanian–Turonian Eagle Ford Shale on and adjacent to the Comanche Platform to determine whether the Eagle Ford Shale has an affinity with the Western Interior, and if so, determine where the transition from Western Interior to open ocean is located. We were also interested in the relationship, if any, between the organic-rich facies of the Eagle Ford and Oceanic Anoxic Event 2 (OAE2). Our work is based on quantitative foraminiferal population counts and associated sedimentary particles (including inoceramid prisms, sand, glauconite, and pyrite grains), calcareous nannofossil assemblages, carbon isotopes, and total organic carbon (TOC) from three sites across a range of paleowater depths: an outcrop in Lozier Canyon in Terrell County, west of Langtry, TX, an outcrop at Bouldin Creek outside of Austin, TX, and Swift Energy's Fasken A #1H core in Webb County, TX.

The highest TOC in the Eagle Ford occurs before the onset of OAE2 (6% at Lozier Canyon, 7% at both Bouldin Creek and the Fasken Core) and then declines steadily through the rest of the section (except for a small increase at the end of OAE2 at Lozier and a fairly large post-OAE2 increase at Bouldin Creek). Nannofossil paleoproductivity indicators (%*Zeugrhabdotus* and %*Biscutum*) track TOC at Bouldin Creek and in the Fasken Core and display similar trends to those observed in the Western Interior Seaway to the north. Benthic foraminiferal abundances increase as TOC decreases and the lithology shifts from laminated black shale to bioturbated light gray shale; low-oxygen-tolerant infaunal *Neobulimina* spp. appear first and gradually increase in abundance; epifaunal benthics appear soon after. This oxygenation trend continues through the OAE2 interval and the upper Eagle Ford contains a diverse epi- and infaunal benthic foraminiferal assemblage and macrofossil assemblage. This trend of decreasing TOC and nannofossil paleoproductivity indicators coupled with increasing benthic foraminiferal abundance and diversity (and seafloor oxygenation) corresponds to rising sea level.

Based on foraminiferal and nannofossil events, TOC trends, and changes in lithology, both platform sites have a strong affinity with the Western Interior, with Lozier Canyon being the most similar; the Fasken Core bears all the characteristics of an open ocean site, except for the fact that peak TOC occurs before OAE2. This suggests that the oceanographic boundary between WIS and Tethys can be placed on the edge of the Comanche Platform. Productivity was likely driven by bathymetry-induced upwelling caused by restriction between the WIS and Tethys during times of low sea level; as sea level rose, upwelling diminished and productivity decreased. This explains why the Fasken Core, adjacent to the platform margin and in the center of this upwelling zone, displays the same TOC trends as the platform sites. Organic carbon content in the seaway was controlled by stratification and enhanced preservation, but this was also reduced by rising sea level, which is why the two areas show parallel trends.

1. Introduction

The Cenomanian and Turonian Stages of the Cretaceous (~100–90 Ma) were a time of elevated tectonic activity, global warmth, high sea level, biotic turnover, and burial of vast amounts of organic carbon in the deep-sea, along continental margins, and in epicontinental seas

* Corresponding author.
E-mail address: chris.lowery09@gmail.com (C.M. Lowery).

http://dx.doi.org/10.1016/j.palaeo.2014.07.025
0031-0182/© 2014 Elsevier B.V. All rights reserved.

(e.g., Schlanger and Jenkyns, 1976; Kauffman, 1977a; Scholle and Arthur, 1980; Arthur et al., 1987; Schlanger et al., 1987; Voigt, 2000; Leckie et al., 2002; Arthur and Sageman, 2005; Jenkyns, 2010; Friedrich et al., 2012).

Changes in biota across the Cenomanian–Turonian boundary are linked to environmental perturbations associated with Oceanic Anoxic Event 2 (OAE2), which caused the evolutionary turnover of, among other things, molluscs (Elder, 1985, 1991), calcareous nannofossils (e.g., Bralower, 1988; Erba, 2004), radiolarians (Erbacher et al., 1996; Erbacher and Thurow, 1997), and benthic and planktic foraminifera (e.g., Leckie, 1985; Kaiho and Hasegawa, 1994; Premoli-Silva and Sliter, 1999; Leckie et al., 2002). OAE2 was a global event that corresponded to widespread burial of organic matter (expressed as black shales) and localized bottom water and photic zone dysoxia or anoxia (e.g., Schlanger and Jenkyns, 1976; Jenkyns, 1980; Arthur et al., 1990; Jenkyns, 2010; Owens et al., 2012), tied to a positive 2‰ excursion in carbon isotopes caused by the enhanced burial of isotopically light organic carbon (e.g., Scholle and Arthur, 1980; Pratt and Threlkeld, 1984; Arthur et al., 1987; Pratt et al., 1993; Tsikos et al., 2004; Jarvis et al., 2006; Sageman et al., 2006; Gale et al., 2008; Barclay et al., 2010; Jarvis et al., 2011).

Current research suggests that OAE2 was caused by increased productivity driven by a rapid influx of micronutrients, likely from seafloor hydrothermal activity related to LIP emplacement (i.e., the Caribbean Large Igneous Province), increased rates of ocean crust production, or increased volcanic CO_2 emissions resulting in global warming and strengthening of the hydrologic cycle, increasing continental weathering and nutrient influx to the oceans (e.g., Leckie et al., 2002; Snow et al., 2005; Barclay et al., 2010; Jenkyns, 2010; Monteiro et al., 2012; van Bentum et al., 2012).

Productivity and enhanced carbon burial associated with this nutrient increase were widespread but not global. A notable exception is the Western Interior Sea of North America, a shallow epicontinental sea that extended from the Canadian Arctic to the Gulf of Mexico, where the onset of OAE2 (based on carbon isotope enrichment) is associated with a transition from dark-gray, organic rich shale to light-gray shale interbedded with limestone (e.g., Kauffman, 1984), a decrease in total organic carbon (e.g., Pratt, 1985), and an increase in planktic and benthic foraminiferal abundance and diversity (e.g., Eicher and Worstell, 1970; Eicher and Diner, 1985; Leckie, 1985) suggesting a local increase in oxygen at a time when large areas of the open ocean were experiencing anoxia and even photic zone euxinia (e.g., Jenkyns, 2010).

Multiple incursions of warm, normal-marine waters from the Tethys made their way into the WIS during its history, coinciding with eustatic transgressions. The largest of these, the transgression of the 3rd-order Greenhorn Cycle, coincides with the onset of OAE2 and a coeval increase in marine macrofossil and microfossil diversity (e.g., Kauffman, 1984; Eicher and Diner, 1985; Elder, 1985, 1989; Leckie et al., 1998). This correlation hints at a sill at the southern aperture of the WIS that isolates the seaway during low sea level, causing stagnation and organic matter preservation. If this is the mechanism causing the WIS to behave differently than the global ocean during OAE2, there should be evidence of a clear transition between the WIS and the open ocean (Gulf of Mexico/Tethys).

The Comanche Platform of Texas may have represented such a sill at the mouth of the Western Interior Seaway. The Cenomanian–Turonian Eagle Ford Shale was draped across this shallow platform and thickens in adjacent basinal and deepwater sections, where it evolved into a major petroleum source rock (Fig. 1). Unlike its well-studied cousin to the north, the Greenhorn Limestone, and in spite of its unique location in the mouth of the Western Interior Seaway, the micropaleontology of the Eagle Ford in Texas has been the focus of surprisingly little research in recent decades (e.g., Pessagno, 1969; Frush and Eicher, 1975; Smith, 1981; Jiang, 1989; Lundquist, 2000; Denne et al., 2014). We investigated carbon isotopes, total organic carbon, and foraminiferal and calcareous nannofossil assemblages in the Eagle Ford Shale from a transect across the Comanche Platform in order to determine 1) whether any part of the Eagle Ford has an affinity with the central Western Interior; 2) where the oceanographic transition from the Western Interior to the Gulf of Mexico is located; 3) what that position may tell us about the influence of sea level in controlling organic matter content in the Western Interior Seaway; and 4) if there is a relationship between the organic-rich facies of the Eagle Ford and OAE2.

2. Geologic setting

2.1. Stratigraphy and micropaleontology of the Western Interior Seaway

The Cenomanian–Turonian interval of the Cretaceous Western Interior Seaway of North America has been the focus of paleoceanographic research for decades (e.g., Eicher and Worstell, 1970; Hattin, 1971; Kauffman, 1977a,b; Pratt and Threlkeld, 1984; Eicher and Diner, 1989; Elder and Kirkland, 1994; Sageman and Arthur, 1994; Leckie et al., 1998; Sageman et al., 1998; West et al., 1998; Meyers et al., 2001, 2005; Sageman et al., 2006; and others). The Global Stratotype Section and Point (GSSP) for the Cenomanian–Turonian Boundary has been placed at the classic exposure at the Rock Canyon Anticline, near Pueblo, CO (Kennedy et al., 2005). Located in the central axial basin of the seaway, the Rock Canyon section occupied a favorable zone where it was not inundated with siliciclastic sediments pouring off the Sevier Highlands to the west or the cratonic interior to the east, and was deeper than the gently sloping hinge-zone of the stable craton to the east (Kauffman, 1984; Sageman and Arthur, 1994; Elderbak et al., in this volume). Its depth and central location meant that it was more likely to be colonized by marine organisms from the Tethyan realm during transgressions and high stands of sea level; Tethyan fauna invaded there first and lingered there the longest, allowing for correlation to other sites ringing the North Atlantic in Europe and North Africa. Foraminiferal studies at Rock Canyon date back to the 1960s (Eicher, 1965, 1966, 1969; Eicher and Worstell, 1970) and have helped form some of our basic notions about foraminiferal trends across the Cenomanian–Turonian boundary (Eicher and Diner, 1985; Leckie, 1985; Fisher et al., 1994; Leckie et al., 1998; Caron et al., 2006). To summarize decades of work, the basic foraminiferal trends at Rock Canyon (and by extension, the southern part of the WIS) are as follows.

The upper Cenomanian Hartland Shale Member of the Greenhorn Limestone, a dark-gray, organic-rich shale, contains an abundant, moderate diversity assemblage of planktic foraminifera, is barren of benthic forams, and corresponds to a time of relative restriction when the seaway was brackish due to poor communication with the Tethys (because of the Comanche Platform in Texas) and freshwater input from the surrounding continent (Kauffman, 1984; Eicher and Diner, 1985; Sageman, 1985; Elderbak et al., in this volume). The contact with the overlying Bridge Creek Limestone Member (commonly known as Bed 63 in Colorado and Marker Bed HL-1 in Kansas; Cobban and Scott, 1972; Hattin, 1975; Elder and Kirkland, 1985) shows a marked increase in planktic foraminifer diversity, including an increase in keeled planktic foraminifera, which characterize normal marine conditions and tend to live in deeper waters (Eicher and Diner, 1985; Leckie, 1985; Leckie et al., 1998; Norris and Wilson, 1998; Petrizzo et al., 2008; Ando et al., 2010). This level also represents an acme of benthic foraminiferal abundance and diversity, labeled the “Benthonic Zone” by Eicher and Worstell (1970). The rapid increase in diversity has traditionally been linked to an incursion of a warm, normal saline, and well-oxygenated water mass from the south associated with the transgressive phase of the Greenhorn Cycle (Eicher and Worstell, 1970; Eicher and Diner, 1985; Elder, 1985; Elder and Kirkland, 1985; Leckie, 1985; Watkins, 1985; Savrda and Bottjer, 1993; Fisher et al., 1994; Leckie et al., 1998). Directly above this interval, benthic foraminifera become scarcer and assemblages are dominated by two species of calcareous taxa: *Neobulimina albertensis* and *Gavelinella dakotensis*. The planktic keeled genus *Rotalipora* goes extinct, and the assemblages are dominated by surface-dwelling planktics, notably the biserial genus *Heterohelix*, an opportunistic taxon that thrives in environments in

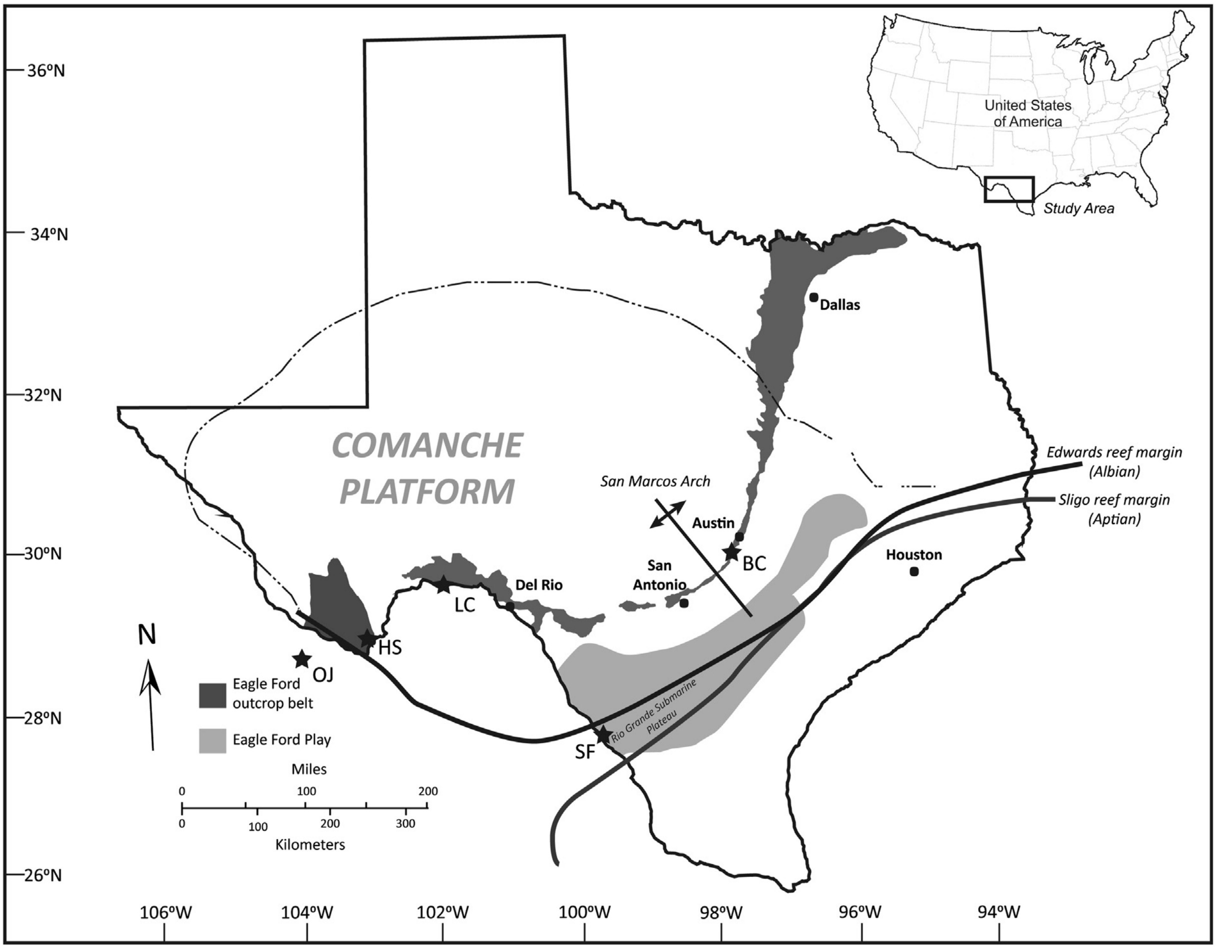

Fig. 1. Map of Texas showing modern Eagle Ford outcrop belt (light gray), extent of the Comanche Platform, relevant paleobathymetric features, and location of study sites (stars). OJ: Ojinaga, Mexico, from Frush and Eicher (1975); HS: Hot Springs locality in Big Bend National Park, from Frush and Eicher (1975); LC: Lozier Canyon; BC: Bouldin Creek; SF: Swift Energy's Fasken Core.
Modified from Donovan et al. (2012).

which other foraminifera struggle (Leckie et al., 1998). These events have been interpreted as the result of the incursion of a low-oxygen water mass from Tethys, where OAE2 was taking hold; this incursion resulted in stratification and deep dysoxia or anoxia in the Western Interior Basin (e.g., Eicher and Diner, 1985; Leckie, 1985; Leckie et al., 1998; Caron et al., 2006). This interval also corresponds to the Cenomanian–Turonian boundary (base of Bed 86 of the Bridge Creek Limestone), which is defined by the first occurrence of the ammonite *Watinoceras devonense* (Kennedy et al., 2005). Above Bed 86, in the lower Turonian, benthic foraminifera remain sparse and of very low diversity while keeled planktics reappear as the low oxygen conditions of OAE2 abate, a trend that continues into the lower part of the middle Turonian Fairport Member of the Carlile Shale (Eicher, 1966; Eicher and Diner, 1985; Leckie et al., 1998; West et al., 1998; Caron et al., 2006).

Calcareous nannofossils are more poorly constrained at Rock Canyon, as important marker species for the Cenomanian–Turonian boundary are reported at many different stratigraphic levels across the boundary interval, possibly reflecting diachroneity of extinctions or problems with rare/poorly preserved specimens (Bralower and Bergen, 1998; Desmares et al., 2007). Biostratigraphic analyses of the exposures at Rock Canyon have been published by Watkins (1985), Bralower (1988), and Corbett et al. (2014). Corbett and colleagues analyzed fifty-eight samples from the Bridge Creek Limestone at Rock Canyon and identified six datums within the OAE2 interval, including the lowest occurrences of *Eprolithus moratus*, *Ahmuellerella octoradiata*, and the highest occurrence of *Corollithion kennedyi*, which are found in the OAE2 interval of the lower Bridge Creek, while the highest occurrence of *Helenea chiastia* and the lowest occurrence of *Quadrum gartneri* bracket the Cenomanian–Turonian Boundary at Bed 86.

The only detailed analysis of calcareous nannofossil assemblages comes from the nearby USGS Portland Core, about 20 miles to the west of Rock Canyon, and has been deemed unreliable for paleoecological interpretation (Burns and Bralower, 1998). Evidence of poor preservation, particularly the dominance of the dissolution resistant species *Watznaueria* (between 40 and 70% of the assemblage), suggests that the more delicate high fertility species may have been preferentially removed. Despite this possible limitation, high fertility species *Zeugrhabdotus* is relatively abundant (~20%) through the middle of the OAE2, suggesting an increase in local productivity. Above this level, organic carbon content increases somewhat in the interbedded shales of the upper Bridge Creek Limestone, at and above the termination of OAE2, but does not return to the levels seen in the Hartland Shale (Pratt, 1985).

2.2. Stratigraphy and micropaleontology of Texas

The Comanche Platform covers a large portion of west Texas and is rimmed by reef buildups; it is bounded to the southeast by the Aptian and Albian Edwards and Sligo reef margins (sometimes collectively called the Stuart City Reef Trend), to the southwest by the Maverick and Sabinas Basins (Donovan and Staerker, 2010), and to the west by the Chihuahua Trough in Mexico (Fig. 1). The Edwards and Sligo reef buildups diverge in southeast Texas, and the deep platform between them is called the Rio Grande Submarine Plateau. The organic-rich mudstones of the Eagle Ford Shale cover the Comanche Platform and form thick deposits in the adjacent basins, which are the centers of the current Eagle Ford oil and gas play. The Eagle Ford is regionally underlain by the lower Cenomanian Buda Limestone (in east Texas the Cenomanian Woodbine Sandstone can be found between the Buda and Eagle Ford) and overlain by the Austin Group.

Geologists were working on the Eagle Ford of west Texas as early as Udden (1907), although it was first described in detail here by Hazzard (1959). A recent boom in drilling activity in the Eagle Ford unconventional gas play in south and east Texas has driven an increase petroleum-oriented research of the west Texas outcrops (e.g., Donovan and Staerker, 2010; Hentz and Ruppel, 2010; Lock et al., 2010; Donovan et al., 2012; Slatt et al., 2012; Eldrett et al., 2014), but most micropaleontological work is decades old.

Pessagno (1969) conducted a regional foraminiferal biostratigraphic study of mid-Cretaceous rocks that defined the Cretaceous planktic foraminiferal zones of the Gulf Coastal Plain. Pessagno sampled a large number of sites in the Eagle Ford outcrop belt, including our study sites at Lozier Canyon and Bouldin Creek; the paper reports mostly marker taxa and no abundance data were recorded, preventing paleoecological interpretation. In far west Texas, Frush and Eicher (1975) studied a series of outcrops in the Big Bend region of Texas and Mexico, on the western flank of the Comanche Platform, where they found an assemblage of foraminifera remarkably similar to what had been described from the U.S. Western Interior, including the "Benthonic Zone." This indicates that assemblages of foraminifera with a Western Interior affinity extend at least as far as the western margin of the Comanche Platform.

Recently published foraminiferal data from Denne et al. (2014) from the Eagle Ford play area on eastern margin of the Comanche Platform, east of our study sites, shows low benthic abundances in the lower Eagle Ford, during intervals of high TOC, and higher abundance and diversity of benthics during the OAE2 interval, which records low TOC.

Smith (1981) published nannofossil data from several roadside outcrops of the Eagle Ford in the vicinity of Del Rio, TX. The biostratigraphic results, however, do not reflect zonal schemes that are now commonly used and many key marker species were not recorded in his study. Nannofossils were only recorded qualitatively and so cannot be used to interpret paleoecological changes. Jiang (1989) performed additional analysis of the Eagle Ford and Austin Chalk at fifteen sites through central and northern Texas around Austin and Dallas, including the West Bouldin Creek site sampled in this paper. No detailed assemblage data were collected in Jiang's study, and while it provides more detailed biostratigraphic information than Smith's earlier work, several key marker taxa were not reported (e.g. *Eprolithus octopetalus*).

2.3. Sequence stratigraphy

The Cretaceous stratigraphy of Texas can be divided into two 2nd-order cycles based on Hill (1887a,b): the Lower Cretaceous Comanchean Sequence, which records the deposition of the carbonate systems that formed the Comanche Platform and includes the Sligo, Pearsall, Glen Rose, Edwards, Georgetown, Del Rio, and Buda formations, and the Upper Cretaceous Gulfian Sequence, a siliceous-dominated sequence that begins with the Eagle Ford and includes the Austin, Anacacho, San Miguel, Olmos, and Escondido formations. The Eagle Ford contains the maximum flooding of the Gulfian sequence, and in fact, represents the maximum flooding of the 1st-order Zuni sequence, which corresponds to the latter half of the Mesozoic (Sloss, 1963). The Eagle Ford itself represents a 3rd-order cycle (called the "Eagle Fordian;" e.g., Pessagno, 1969), which is equivalent to the 3rd-order Greenhorn Cycle in the WIS (Kauffman, 1984), making it coeval with the Greenhorn Limestone described above. Donovan et al. (2012), working primarily from Lozier Canyon and correlating to surrounding sites and the east Texas subsurface, divided the Eagle Ford into four members (Lozier Canyon Member, Antonio Creek Member, Scott Ranch Member and Langtry Member; Fig. 2), each of which corresponds to a 4th-order sequence. The definitions and rational for these members/sequences are discussed in detail by Donovan et al. (2012) and are summarized below.

Donovan and colleagues demonstrated the similarities between the east Texas subsurface and west Texas outcrop area by correlating units between the two with geochemical and petrophysical data (e.g., gamma ray logs). They base their four members around four mudstone-rich zones, which they interpret and marine condensed intervals. These highstands are bounded by five sequence boundaries. The lowermost is the contact between the Buda Limestone and Eagle Ford Shale, a regional unconformity that represents the transition between the Comanchean and Gulfian sequences (Sloss, 1963). A near-shore, shallow water sequence at the base of the Eagle Ford, with hummocky cross stratification and disarticulated oyster beds, slowly gives way to an anoxic, offshore mudstone facies. A sequence boundary, also delineating the boundary between the Lozier Canyon and Antonio Creek members, is placed after the peak TOC, corresponding to an increase in grainstone beds and %$CaCO_3$; the corresponding maximum flooding surface is placed at an inflection point in the natural gamma ray profile. The sequence boundary between the Antonio Creek and Scott Ranch Members is placed at a distinct lithologic change from dark gray, organic-rich mudstone to light gray calcareous shale interbedded with limestone. The maximum flooding surface is placed near the top of this interval at a slight increase in TOC, and is immediately followed by a sequence boundary. This boundary is marked by a color transition from light gray shale interbedded with grainstones to tan-colored, highly bioturbated marls and marked by a lag bed with pebble-sized rip-up clasts. This Langtry Member is characterized by a coarsening upward sequence with increasing wave-ripple grainstones toward the contact with the Austin Chalk, with rip-up clasts again marking the boundary to wackestones interbedded with thin black mudstones of the basal Austin Chalk.

3. Locations and methods

3.1. Study sites

We examined a transect of three sites across the Comanche Platform for planktic and benthic foraminiferal assemblages, calcareous nannofossil assemblages, total organic carbon (TOC) and carbon isotopes from the Eagle Ford Shale. These data come from Lozier Canyon in Terrell Co., TX; Bouldin Creek, in Travis Co., TX, adjacent to a structural high called the San Marcos Arch; and from Swift Energy Company's Fasken A #1H Core, off the southeastern edge of the Comanche Platform on the Rio Grande Submarine Plateau, a deeper water site between two early Cretaceous reef margins (Fig. 1). We compare these results to published foraminiferal data of Frush and Eicher (1975) from the western slope of the Comanche Platform at Ojinaga, Mexico, and the far west Comanche platform at Hot Springs in Big Bend National Park.

3.1.1. Lozier Canyon

Lozier Canyon, a "seasonal" (every few years in west Texas) river bed a few miles from the Mexican border and about nine miles west of the hamlet of Langtry, in Terrell County, TX, on private land leased to BP, contains a complete exposure of the Eagle Ford Shale on a natural, nearly vertical 55 m high face (Fig. 2). Samples were collected at roughly half-meter intervals from freshly exposed rock. Detailed discussion of regional Eagle Ford geology and detailed sedimentological descriptions of the Lozier Canyon section from our fieldwork can be found in Donovan et al. (2012), but briefly: the Eagle Ford at Lozier Canyon is divided into four members. The Lozier Canyon Member is comprised of light gray interbedded mudstones and grainstones with individual stacked beds of wave ripples and hummocks, overlain by laminated dark gray organic-rich mudstones alternating with thin, grainstone-prone

Please cite this article as: Lowery, C.M., et al., Foraminiferal and nannofossil paleoecology and paleoceanography of the Cenomanian–Turonian Eagle Ford Shale of southern Texas, Palaeogeogr. Palaeoclimatol. Palaeoecol. (2014), http://dx.doi.org/10.1016/j.palaeo.2014.07.025

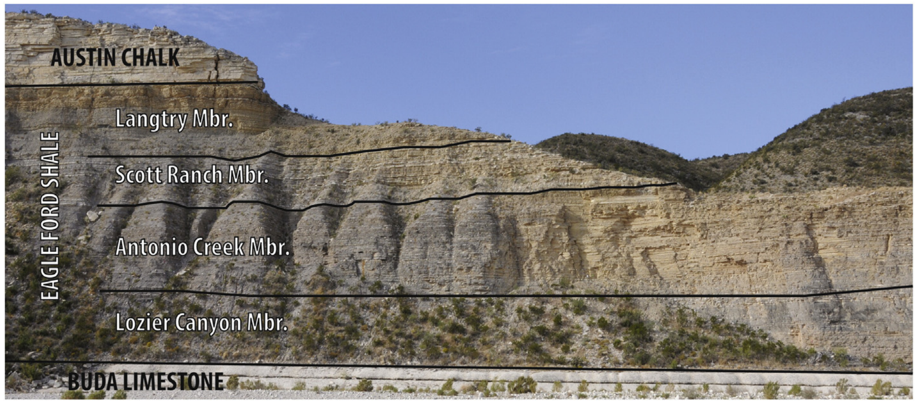

Fig. 2. Photograph of Lozier Canyon locality showing typical stratigraphy of the Eagle Ford Shale, including the underlying lower Cenomanian Buda Limestone, the organic-rich lower unnamed shale and Middle Shale Member, the upper unnamed shale member, which has more interbedded limestones and corresponds to Oceanic Anoxic Event 2, the Langtry Member, and the overlying Austin Chalk.

limestones. The Antonio Creek Member is also a dark gray organic-rich mudstone alternating with grainstone-prone limestones, and is mainly differentiated by the occurrence of multiple bentonites beds throughout the member. The Scott Ranch Member consists of light-gray packstone–grainstone bedsets and bioturbated calcareous mudstones; the lithologic contact with the underlying Antonio Creek Member is abrupt, with a prominent grainstone and obvious color change. The Langtry Member is composed of highly bioturbated yellow marls overlain by yellow-ocre grainstones and mudstones, with wave ripples and small hummocks. Lozier Canyon is located on the southwestern part of the Comanche Platform.

Pessagno (1969) sampled Lozier Canyon at Highway 90 (which he described as a "classic exposure" of the Eagle Ford) as part of his regional biostratigraphic study. According to photographs included in his work, we sampled the same sections of the same exposure. He sampled at 10- to 20-foot (3–6 m) intervals at Lozier (for a total of eight samples), and so provides a coarse biostratigraphy. He described a paraconformity somewhere between 127 and 160 ft (~39–49 m). Samples below this paraconformity contain an assemblage of foraminifera that he found assignable to the *Rotalipora cushmani* Zone, and he assigned the samples above to the *Helvetoglobotruncana helvetica* Zone. An examination of Pessagno's original picked slides at the Cushman Collection at the Smithsonian Natural History Museum didn't reveal any *H. helvetica*; it is unclear whether he actually found this taxon in these samples or based the zonal assignment on the absence of *Rotalipora* spp. or by occurrence of other early Turonian planktic species. Pessagno assigned the Austin Chalk exposed at Lozier to the now-defunct *Marginotruncana renzi* Zone.

3.1.2. Bouldin Creek

Bouldin Creek is a small stream located in Austin, with access near the intersection of S. 7th St. and W. Monrose St., whose banks contain vertically incomplete exposures of the Eagle Ford Group, locally mapped as the Pepper Shale, the Cloice Shale, the Bouldin Flags Formation, and the South Bosque Shale. Our samples come from a 10.7 m section that includes the upper Cloice Member, comprised of laminated calcareous mudstone; the Bouldin Flags Member, comprised of interbedded mudstones and grainstone with occasional wave ripples and common bentonites; the South Bosque Member, which is comprised of laminated calcareous mudrock; and the overlying Atco Member of the Austin Chalk. We took a few samples from a separate outcrop of the Buda Limestone and basal Pepper Shale a short distance downstream, but these turned out to be very poorly preserved and barren of foraminifera and nannofossils. The Austin area is perched in the center of the Comanche Platform on the eastern side of the San Marcos Arch, an area of very gradual tectonic uplift during the late Cretaceous (Sohl et al., 1991; Donovan et al., 2012).

The Bouldin Creek outcrops represent a presumably identical stratigraphic package to that found in the nearby ACC #1 Core taken 11.2 miles to the north-northeast of Bouldin Creek and stored with the Bureau of Economic Geology in Austin. Calcareous nannofossils reported herein are from the ACC core, but not enough core material was available for foraminiferal, stable isotope, or TOC analyses, which were taken from Bouldin Creek. We were able to retrieve excellent foraminiferal material from the outcrop (the best preserved of our three study sites), but the degraded nature of the exposure meant that many of the sedimentological features noted in the core are not visible in outcrop (especially the "Rubble/Condensed Zone" at the base of the Austin).

Pessagno (1969) also examined the Eagle Ford around Austin, TX, including our Bouldin Creek section, but his seven samples from this site only split the *Rotalipora cushmani* and *Helvetoglobotruncana helvetica* zones, lumping all of the upper Eagle Ford and lower Austin into the latter. A more detailed paleoecological study by Lundquist (2000) examined the Eagle Ford, Austin, and Taylor Groups in central Texas, including the outcrop at Bouldin Creek and several subsurface cores. He documented an open ocean assemblage of planktics in the Pepper Shale (Fig. 3) and a predominance of agglutinated benthics. The agglutinates are less common in the Cloice and Bouldin Flags (equivalent to the Antonio Member elsewhere), and biserial taxa become more prevalent in the assemblage. Above a Cenomanian/Turonian unconformity, the South Bosque Shale is dominated by biserial planktics and infaunal benthics, suggesting a more stressed environment. These changes were interpreted to have come about because of the displacement of a Boreal water mass in the Cenomanian (evidenced by the agglutinated benthics) by warm, dysoxic Tethyan waters. Lundquist interpreted an oceanic front separating these two water masses that moved across the Austin area several times before Tethyan waters came to dominate during the Turonian. Lundquist also documents the occurrence of a "Rubble Zone" at the top of the Eagle Ford, containing abundant phosphate nodules, glauconite, and fish debris, presumed to represent an erosional surface below the Austin Chalk.

Jiang's (1989) nannofossil analysis of the Eagle Ford and Austin Chalk includes the Bouldin Creek site. Jiang suggested that the HO of *Helenea chiastia* and the presence of *Lithraphidites acutum* and *Lithraphidites alatus* indicate that the Cloice/Waller and Bouldin Creek members are upper Cenomanian, while the total range of *Eprolithus moratus* suggests that the South Bosque Member is Turonian. The LO of *Lithastrinus septenarius*, *Marthasterites* spp., and *Liliasterites* spp. imply a late Turonian to early Coniacian age for the deposition of the basal Atco Member of the Austin Chalk.

Please cite this article as: Lowery, C.M., et al., Foraminiferal and nannofossil paleoecology and paleoceanography of the Cenomanian–Turonian Eagle Ford Shale of southern Texas, Palaeogeogr. Palaeoclimatol. Palaeoecol. (2014), http://dx.doi.org/10.1016/j.palaeo.2014.07.025

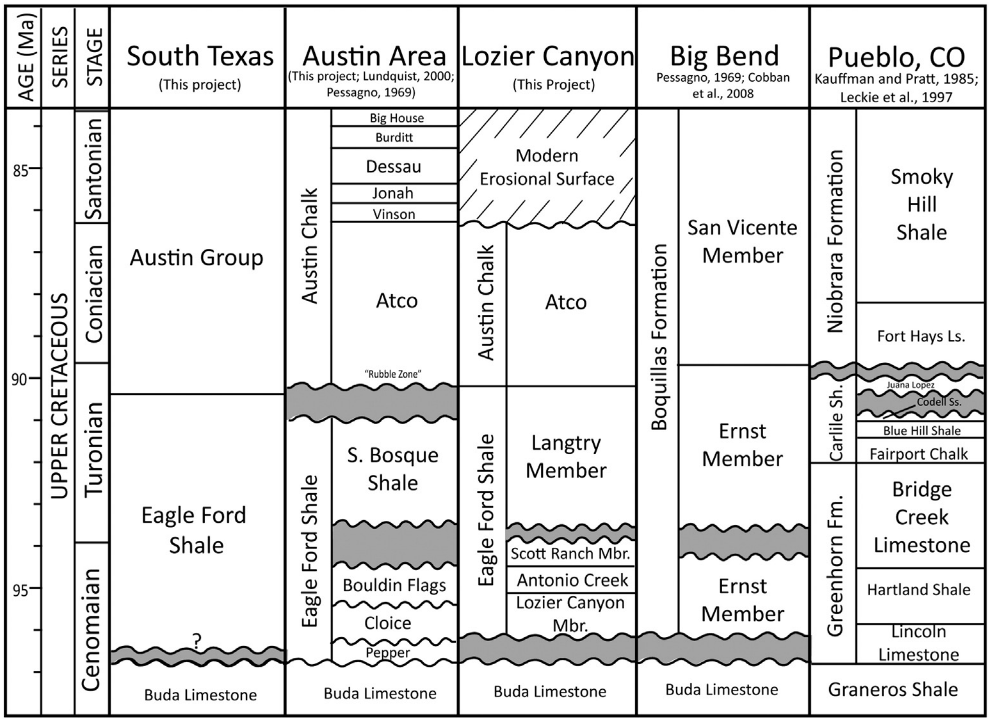

Fig. 3. Chronostratigraphic correlation between south Texas and the Cenomanian–Turonian GSSP in Pueblo, Colorado. Correlation and stage boundaries based on our own data, as well as figures and descriptions from Pessagno (1969), Kauffman and Pratt (1985), Leckie et al. (1997), Lundquist (2000), and Cobban et al. (2008). Ages based on Gradstein et al. (2012).

3.1.3. Fasken Core

Swift Energy's Fasken A #1H Core is located in Webb County on the Rio Grande Submarine Plateau, off the eastern margin of the Comanche Platform. The cored interval available for study is 159.3 m thick with a base at 2993.1 m below the surface, and includes the very top of the Buda Limestone (2.3 m), the complete Eagle Ford Shale (119.0 m), and the lower Austin Chalk (38.0 m); samples were made available at roughly 2-meter intervals. Subsurface log picks of the Austin–Eagle Ford contact are inconsistent, however, and sometimes the Langtry Member of the Eagle Ford is lumped with the Austin; it is unclear if the base of the Austin was picked correctly in the Fasken. The Eagle Ford consists entirely of black, laminated shale with occasional pyrite nodules. Lithologic variability can be best seen from the gamma ray log, which shows a "marker bed" at the top of the Middle Shale Member that is identical to that seen from outcrop gamma ray at Lozier Canyon.

3.2. Foraminiferal methods

For foraminiferal population analysis, bulk rock samples were crushed to roughly centimeter chunks and soaked in a 3% solution of Miramine (a surfactant similar to Quaternary-O) and water for at least 24 h, then washed over a 63-μm sieve and dried in an oven. Dried samples were split to obtain at least 300 individuals when possible (some samples did not yield 300 foraminifera), which were then picked and counted. Individuals that could not be identified to the genus level are categorized as "planktic spp." or "benthic spp." In poorly preserved intervals, these individuals made up a significant part of the assemblage. Because of the importance of planktic–benthic ratios to this study, and because unidentifiable foraminifera were nearly always planktic, we have included these individuals in the count totals. For nearly every "planktic spp." it was possible to determine whether the test was coiled or biserial, and so this information is included in our morpho-group proportions below (completely unidentifiable individuals are excluded). Significant sedimentary particles found in the foram wash were also counted. These include macrofossil debris (fish debris, inoceramid prisms, and echinoid spines), pyrite grains, sand grains, and glauconite grains, and are here displayed as a percentage relative to the total population of foraminifera.

For biostratigraphic purposes, we define the key Cretaceous planktic foraminiferal zones present in our study interval (after Caron, 1985; Gradstein et al., 2012; Huber and Petrizzo, 2014).

3.3. Calcareous nannofossil methods

Calcareous nannofossils were studied using a Zeiss Photoscope III at a total magnification of 1250× using cross-polarized light, plane light, phase contrast, and through a one-quarter λ mica plate. Slides from outcrop and core samples were prepared using the double slurry and settling methods detailed by Geisen et al. (1999) and Watkins and Bergen (2003), respectively. Calcareous nannofossil biostratigraphy is addressed in detail by Corbett et al. (2014).

Several semi-quantitative methods for interpreting preservation are frequently used for Cretaceous material based on work by Roth and Krumback (1986) and Williams and Bralower (1995). Roth and Krumback (1986) and Erba (1992) note that *Watznaueria* negatively correlates to species richness in successions of poorly preserved material. Increasing abundances of *Watznaueria* indicate that increasing numbers of species are likely to have dissolved away. Thierstein (1981) and Roth and Krumback (1986) suggest using 40% relative abundance of *Watznaueria* as a cut-off for samples that are likely altered from their original assemblage composition. A strong correlation between lower richness and higher relative abundance of *Watznaueria* is also used to imply diagenetic overprinting of an assemblage (Roth and Krumback, 1986; Tantawy, 2008).

3.4. Geochemistry methods

Stable isotopes of carbon are commonly measured from either inorganic carbonate crystals (i.e., "bulk carbonate") or organic matter, the latter being far more isotopically depleted. Although both techniques

Please cite this article as: Lowery, C.M., et al., Foraminiferal and nannofossil paleoecology and paleoceanography of the Cenomanian–Turonian Eagle Ford Shale of southern Texas, Palaeogeogr. Palaeoclimatol. Palaeoecol. (2014), http://dx.doi.org/10.1016/j.palaeo.2014.07.025

faithfully capture trends in the global carbon cycle, bulk rock isotopes can sometimes be offset between shales and limestones, which appear to be more susceptible to post-depositional alteration (e.g., Pratt and Threlkeld, 1984). For this reason, we only report samples from shales and exclude limestones in our $\delta^{13}C_{carbonate}$ analyses.

Bulk rock isotope samples were obtained by grinding roughly a gram of sample into a fine powder to ensure even dissolution. For $\delta^{13}C_{carbonate}$, this powder was reacted with phosphoric acid at 70 °C to liberate CO_2 gas in a Kiel III automated carbonate preparation device inline with a ThermoElectron Delta-Plus mass spectrometer at the University of Massachusetts, Amherst. Values are reported relative to the Vienna Pee Dee Belemnite (VPDB) standard via regular calibration to an internal laboratory standard. Precision is better than 0.03‰ for $\delta^{13}C$.

Organic carbon isotope samples were decalcified using 1 N hydrochloric acid and rinsed with deionized water until a neutral pH was reached. Decalcified samples were dried, weighed into silver boats and then analyzed for total organic carbon (%TOC) using a Costech ECS 410 elemental analyzer coupled to a Thermo-Finnigan V Advantage Isotope Ratio Mass Spectrometer at the University of Massachusetts. $\delta^{13}C_{org}$ data were standardized to VPDB using internal standards. Crushed rock samples (approximately 1 g each) were also sent to GeoMark Research, Inc. for TOC analysis.

4. Results

4.1. Geochemistry

4.1.1. Stable isotopes

Both bulk rock and organic carbon isotope records show a strong positive excursion of 2–3‰ $\delta^{13}C$ VPDB at Lozier Canyon and in the Fasken Core (Fig. 4). There is no carbon isotope record for the Bouldin Creek outcrop. At Lozier the excursion begins at the base of upper unnamed shale member (28.6 m; "marker bed" of Donovan et al., 2012) with an initial positive excursion, followed by a brief recovery to pre-excursion values around 32.0 m, and a longer positive excursion from 32.0 to 39.6 m, ending abruptly at the top of unnamed shale. This general structure in the data has been reported at many sites globally with an initial enrichment ("A"), a brief recovery ("B"), and a sustained plateau ("C") as first described by Pratt and Threlkeld (1984) and subsequently found globally (e.g., Jarvis et al., 2006). In the Fasken, the excursion starts between 2938.1 and 2935 m, at the top of what is labeled in gamma ray logs as a "marker bed," correlative to the "marker bed" at Lozier Canyon (Donovan et al., 2012). Unfortunately, due to poor sample resolution, we cannot resolve the structure of the curve. Orbital solutions for rhythmic bedding from the USGS Portland Core in Colorado by Sageman et al. (2006) put the duration of OAE2 at 847–885 kyr. Since the Fasken section is conformable, we can use this to estimate a sedimentation rate of 1.33 cm/kyr (±0.47 cm) at this location during the OAE interval.

4.1.2. TOC

The highest TOC at Lozier Canyon (Fig. 5A) can be found in the lower unnamed shale member, where values exceed 6 wt.%. TOC is generally low through the Middle Shale Member and the initial part of OAE2 (~1 wt.% hydrocarbon). The "C" part of the carbon isotope excursion in the upper unnamed shale corresponds to a second, smaller peak in TOC (>2 wt.%), before dropping to almost zero in the Langtry Member.

The Eagle Ford at Bouldin Creek contains two intervals enriched in TOC (Fig. 5B). The lower and larger (~7 wt.%) is in the basal two meters of the outcrop in the Pepper and Cloice Shales. The second covers most of the South Bosque Shale above the lower unconformity and the

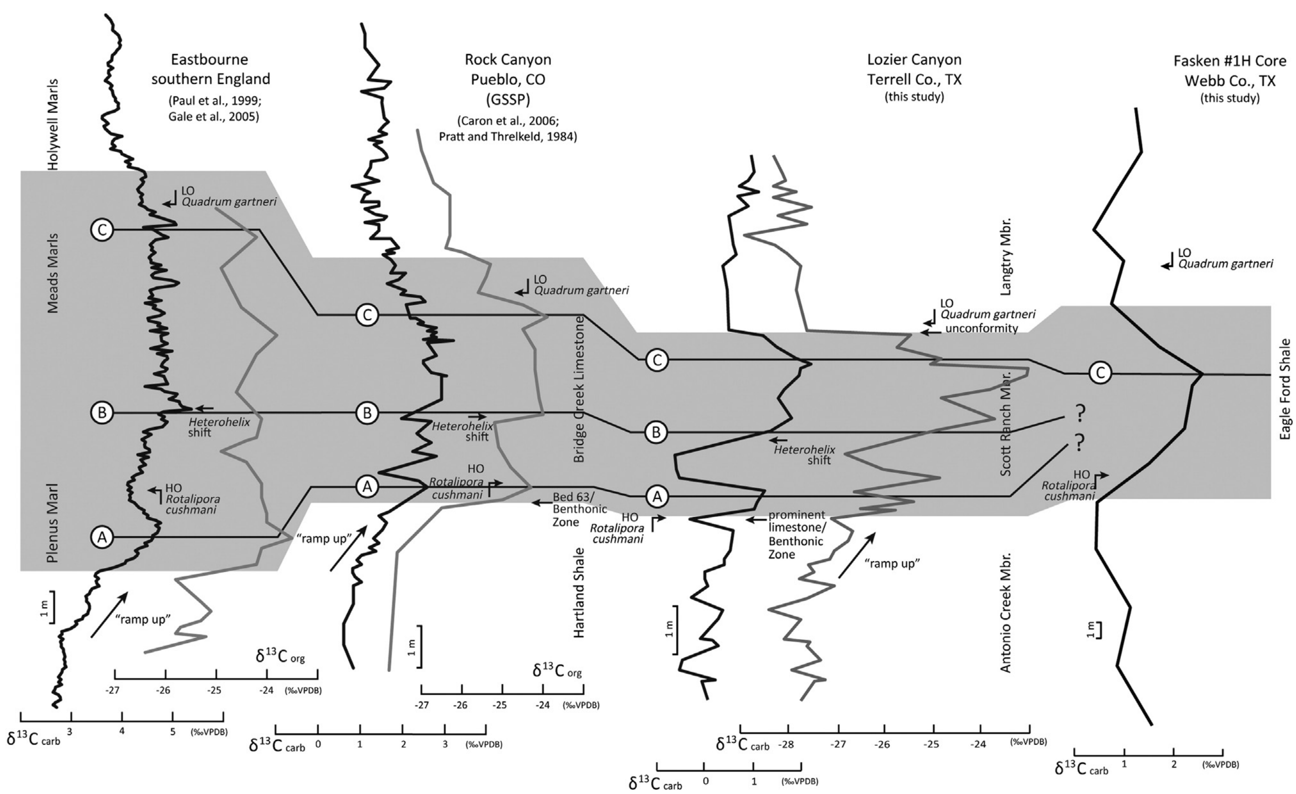

Fig. 4. Comparison of bulk carbonate (black line) and organic (gray line) carbon isotope values during OAE2 from Eastbourne, England (carbonates: Paul et al., 1999; organics: Gale et al., 2005), the C–T GSSP at Rock Canyon, CO (carbonates: Caron et al., 2006; organics: Pratt and Threlkeld, 1984), Lozier Canyon, TX (this study) and the Fasken Core in Webb CO, TX (this study). The general structure of the OAE excursion, including the initial enrichment ("A"), a brief recovery ("B"), and a sustained plateau ("C"), first described by Pratt and Threlkeld (1984) is highlighted by lines of correlation. Gray shaded area corresponds to OAE2. Note how carbon isotopes "ramp up" prior to the event, coincident with the Benthonic Zone in Pueblo and Rock Canyon.
Modified from Jarvis et al. (2006).

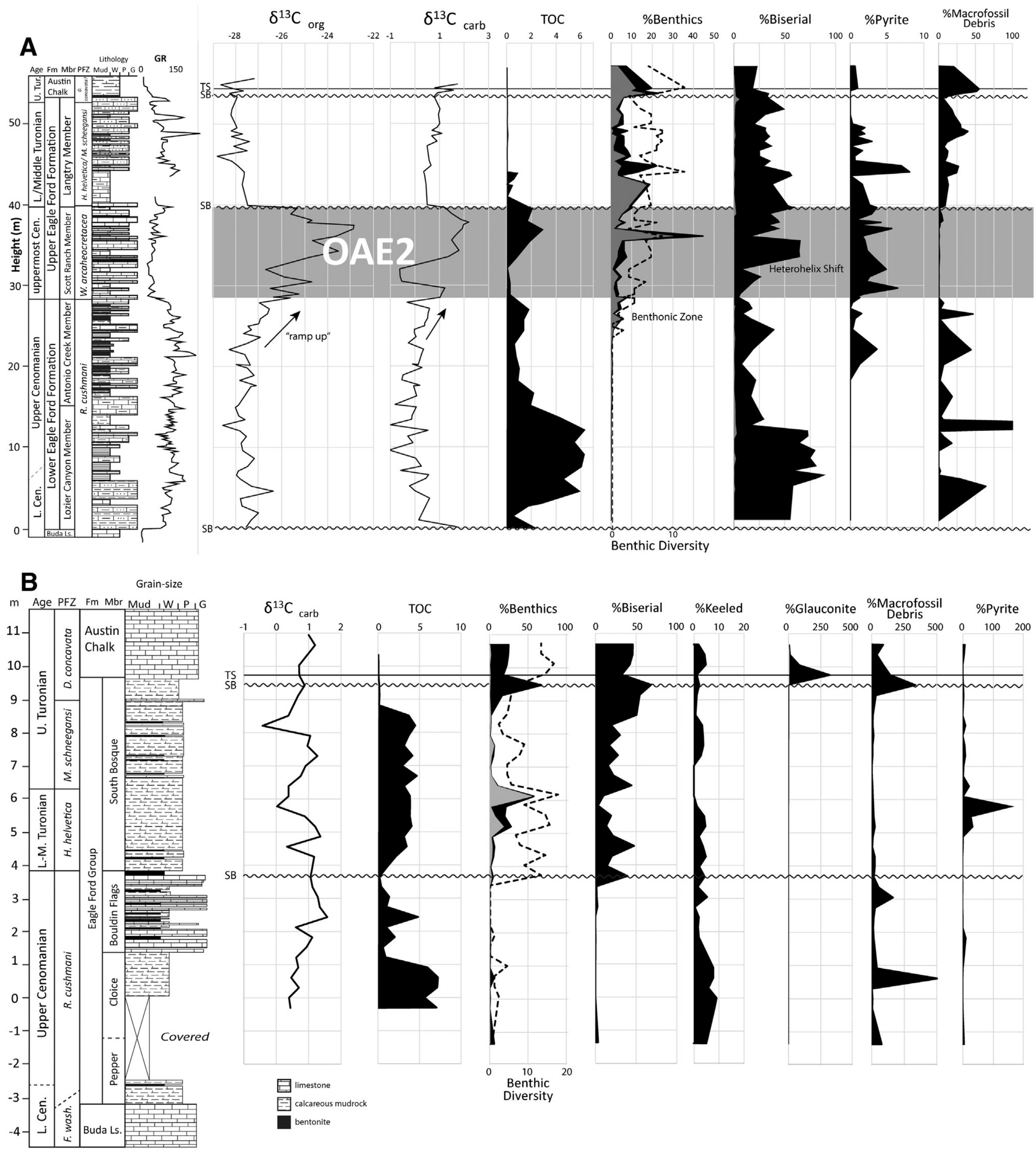

Fig. 5. (A) Geochemical and foraminiferal assemblage data from the Lozier Canyon outcrop in Terrell Co., TX, including total gamma ray, organic carbon isotopes, bulk carbonate carbon isotopes, total organic carbon (TOC), %benthics, %infaunal benthics (light gray inset), benthic simple diversity (i.e., number of species; dashed line) %biserial planktics, %keeled planktics (light gray inset), %macrofossil debris (defined as inoceramid prisms, echinoid spines, and fish debris) and %pyrite grains. Sedimentary particle counts plotted as a percentage vs. total foraminifera. Major regionally defined sequence boundaries (SB), maximum flooding surface (MFS) and transgressive surface (TS) are notated on the plot. Gray bar delineates OAE2. See lithologic key in (B). (B) Geochemical and foraminiferal assemblage data from the Bouldin Creek outcrop in Travis Co., TX, including bulk carbonate carbon isotopes, TOC, %benthics, %infaunal benthics (light gray inset), benthic simple diversity (dashed line) %biserial planktics, %keeled planktics, %glauconite, %macrofossil debris (defined as inoceramid prisms, echinoid spines, and fish debris), and %pyrite grains. Sedimentary particle counts are plotted as a percentage vs. total foraminifera. Major regionally defined sequence boundaries (SB), maximum flooding surface (MFS) and transgressive surface (TS) are noted on the plot. Note that planktic foram zones skip the latest Cenomanian *Whiteinella archaeocretacea* Zone and that there is major positive excursion in the carbon isotopes, both of which indicate an unconformity at the base of the Turonian. (C) Geochemical and foraminiferal assemblage data from Swift Energy's Fasken A #1H core in Webb Co., TX, including total gamma ray, bulk carbonate carbon isotopes, TOC, %biserial planktics, %keeled planktics %benthics, benthic simple diversity (dashed line) %infaunal benthics (not present), sand grains, and %radiolarians. Radiolarians are plotted as a percentage vs. total foraminifera. Gray bar delineates OAE2.

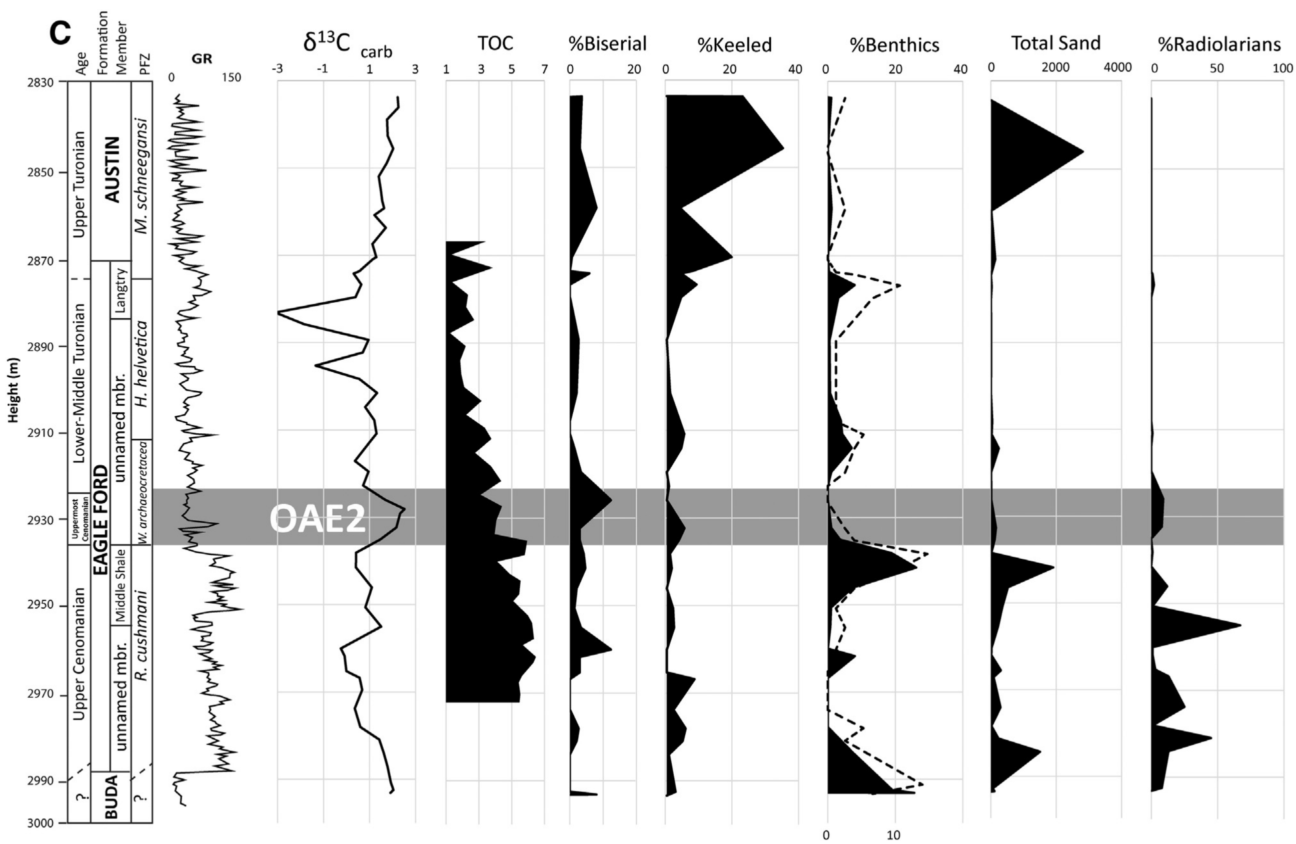

Fig. 5 (*continued*).

"Rubble Bed" at the basal Austin, between 5.1 and 9.5 m, with values averaging ~4 wt.%.

TOC in the Fasken core (Fig. 5C) steadily decreases from a peak of 6.4 wt.% just above the Buda at 2970 m below the surface, to a minimum of 1.82 wt.% at 2901.5 m, about 25 m above the end of OAE2. TOC is variable in the Austin Chalk, ranging from 1.3 to 3.7 wt.%.

4.2. Foraminifera

4.2.1. Planktic foraminifera

The lower five meters of the Eagle Ford at Lozier Canyon (Fig. 5A) is almost completely barren of foraminifera. Washed samples at the very bottom of the formation are almost entirely comprised of dolomite rhombs. Some cross-stratified sandy beds contain planktic foraminifera in thin section (not recovered in the wash and therefore not reflected in the counts), which were likely transported with the sand during storm events. The upper portion of the Lozier Canyon Member contains rare, poorly preserved planktic foraminifera, mainly of the genus *Heterohelix*, and abundant inoceramid prisms. This interval frequently did not yield 300 foraminiferal specimens, although this may be due to preservational factors. The upper 10 m of the Lozier Canyon Member yields more abundant foraminifera, but the assemblage is dominated by small specimens of *Heterohelix*. The Antonio Creek Member records a transition to an assemblage dominated by the trochospiral genus *Hedbergella* (~80%). Keeled taxa (i.e., *Rotalipora* spp. and *Praeglobotruncana* spp.) are very rare but present throughout. The keeled genus *Rotalipora* and planispiral species *Globigerinelloides bentonensis* have their highest occurrence in the uppermost sample of the Antonio Creek Member (28.6 m). Keeled planktic foraminifera are completely absent from the Scott Ranch, while the planktic assemblages shift from trochospiral *Hedbergella*-dominance to biserial *Heterohelix*-dominance at 33.5 m. Interestingly, this interval also sees a nearly complete disappearance of inoceramid prisms (although rare inoceramids can be found in the outcrop). Keeled planktic foraminifera become present again in the base of the Langtry Member, while the percentage of *Heterohelix* in the assemblage decreases, but remains relatively high (>50%). Inoceramid prisms also return at this level. The percentage of the biserial planktic *Heterohelix* drops below 50% in the upper Langtry Member, and is replaced by a relatively diverse assemblage of *Hedbergella*, *Whiteinella* and keeled planktics including *Dicarinella* and *Marginotruncana*.

The lower two members of the Eagle Ford at Bouldin Creek (Fig. 5B) contain assemblages dominated by trochospiral planktics, notably *Hedbergella delrioensis*, *Hedbergella simplicissima*, and *Hedbergella planispira*. The keeled species *Praeglobotruncana delrioensis* is a minor but important component of the assemblage in the lower Eagle Ford. The most striking feature of the Bouldin Creek outcrop is the lowest occurrence (LO) of *Helvetoglobotruncana helvetica* in the basal South Bosque, directly above the highest occurrence (HO) of *Rotalipora cushmani* at the top of the Bouldin Flags Member, suggesting an unconformity that has entirely erased the *Whiteinella archeocretacea* Zone. *Heterohelix*, which is dominant in the lower Eagle Ford at Lozier, is nearly absent here until the South Bosque Member. It shows highly variable abundance, but reaches an acme in the upper South Bosque at 9.4 m, concurrent with a spike in macrofossil debris and epifaunal benthic foraminifera (see below) suggesting a sea level lowstand. This is immediately followed at 9.8 m by a decline in %biserial, %benthics, and %macrofossil debris, and a major peak in glauconite, which is extremely rare in the rest of the South Bosque. This interval corresponds to a "rubble zone" (that is not evident in outcrop but very evident under the microscope as a flood of glauconite and macrofossil debris) in what is labeled as the basal Austin Chalk in the nearby ACC #1 core.

Swift Energy's Fasken #1 core (Fig. 5C), located off the Comanche Platform on the Rio Grande submarine plateau, has intermittent preservation of foraminifera throughout the Eagle Ford. This is probably related to depth of burial (the Eagle Ford is ~2870–2990 m below the surface). Preservation is generally the poorest in the middle Eagle Ford, but varies

Please cite this article as: Lowery, C.M., et al., Foraminiferal and nannofossil paleoecology and paleoceanography of the Cenomanian–Turonian Eagle Ford Shale of southern Texas, Palaeogeogr. Palaeoclimatol. Palaeoecol. (2014), http://dx.doi.org/10.1016/j.palaeo.2014.07.025

from sample to sample throughout. The best preserved samples have mostly pyritized foraminifera, which preserved detailed features (pores, aperture, etc.). Samples with no foraminifera (24 out of 69) are excluded from the population analysis because we suspect this is a result of poor preservation and not a true lack of foraminifera. Other workers have encountered similar preservation issues working in producing Eagle Ford wells; Denne et al. (2014) found foraminifera in thin section in intervals where the wash was barren.

Planktic foraminiferal populations in the Fasken are dominated by inflated trochospiral taxa, notably *Hedbergella delrioensis* and *Whiteinella* spp. Keeled genera (*Praeglobotruncana* and *Rotalipora* in the lower Eagle Ford and *Dicarinella* and *Marginotruncana* in the upper Eagle Ford and Austin Chalk) generally make up ~5% of the assemblage throughout the Eagle Ford, although they greatly increase in abundance (20–30%) in the Austin. The biserial genus *Heterohelix* is rare (~5% with a few peaks at above 10%) throughout the section.

The Fasken is the only study site where we recognize radiolarians. Radiolarians are most common in heavily pyritized samples, so their individual peaks may be artifacts of preservation, but they are only present before OAE2, with a single sample containing a small peak at the end of the OAE2 isotope excursion.

4.2.2. Benthic foraminifera

The lower Eagle Ford at Lozier Canyon (Fig. 5A) contains almost no benthic foraminifera (except for a single *Gavelinella* in the Lozier Canyon Member) until the upper part of the Antonio Creek Member (~26 m), where a sustained, though weak, benthic population made up almost entirely of the infaunal genus *Neobulimina* takes hold. This interval, which we suspect is correlative to the "Benthonic Zone" at Big Bend and in the WIS (Frush and Eicher, 1975), continues throughout the Scott Ranch Member and coincides with OAE2. At 43 m, the percentage of benthic individuals in the population reaches an acme of 36% before returning to background levels in the next sample. Brief pulses of benthic foraminiferal abundances ("repopulation events," e.g., Friedrich, 2010) have been reported elsewhere during the OAE2 interval, such as the Demerara Rise in the tropical Atlantic (ODP Leg 207; Friedrich et al., 2006). If other records are an indication, it is likely that there are other spikes in the benthic population that are not observed in our half-meter resolution; we do not find this acme event in our other Texas study sites. The benthic assemblage is dominated by the infaunal genus *Neobulimina*. The lower Langtry Member shows increased percent benthic values of 10–20%, still nearly entirely composed of *Neobulimina albertensis and Neobulimina canadensis*. The upper Langtry shows an overall decrease in %benthic with values oscillating between 5 and 10%, but the benthic population diversifies to include more epifaunal taxa, notably *Planulina* and *Gavelinella*.

Benthic foraminifera are nearly absent from the lower members of the Eagle Ford at the Bouldin Creek outcrop (Fig. 5B), with the exception of a single sample in the basal Pepper, a single sample in the upper Cloice, and a single *Gavelinella* sp. in the Bouldin Flags. Because the OAE2 interval is completely missing at Bouldin Creek we cannot identify a "Benthonic Zone." However, both infaunal (*Neobulimina albertensis* and *Neobulimina canadensis*) and epifaunal benthics (*Gavelinella dakotensis*, *Gavelinella petita*, and *Planulina* spp.) become consistently present above the unconformity in the lower Turonian. There are two benthic foraminiferal acme events. The first, 58% of the total foraminiferal assemblage, at 6.1 m, is almost exclusively the infaunal taxon *Neobulimina*, although the sample immediately below (21% benthics) contains exclusively epifaunal species, dominated by *G. dakotensis*. The second benthic acme (9.4 m) is coincident with a peak in biserial planktics and macrofossil debris, and is immediately followed by a peak in glauconite. This event is stronger than the first (68% benthics), and contains exclusively epifaunal taxa dominated (173 out of 204 individual benthics) by *G. petita*.

The Fasken core (Fig. 5C) contains trends that are very different from the Eagle Ford on the Comanche Platform. Benthic foraminifera show several peaks, but the largest are in the lower Eagle Ford, below OAE2. With the exception of three specimens of *Bulimina fabilis* and a single *Bifarina* sp., the benthic population is composed exclusively of epifaunal taxa. The benthic assemblage is diverse throughout, but is generally dominated by *Lingulogavelinella* in the acme events (in some cases, the populations of other benthic species stay constant, and a flood of *Lingulogavelinella* spp. cause the %benthics to increase substantially).

No agglutinated foraminifera were found in our study sites. This is in contrast to Lundquist (2000), who found abundant agglutinated benthics in the Pepper and Cloice shales near Austin. It is likely that weathering of the Bouldin Creek outcrop (where we only recovered one poorly-preserved sample from each the Pepper and the Cloice) destroyed the agglutinates, and that if we had access to core materials we could have duplicated Lundquist's (2000) results in these members.

4.3. Calcareous nannofossils

The use of calcareous nannofloral assemblages for interpreting surface water fertility is well documented (Burns and Bralower, 1998; Gale et al., 2000; Erba, 2004; Eleson and Bralower, 2005; Watkins et al., 2005; Hardas and Mutterlose, 2007; Linnert et al., 2010, 2011). Two genera in particular, *Biscutum* and *Zeugrhabdotus*, are believed to indicate mesotrophic conditions and high fertility based on their high abundance in areas of upwelling and elevated organic matter (Roth, 1981; Roth and Bowdler, 1981; Roth, 1986; Roth and Krumback, 1986; Watkins, 1986; Premoli-Silva et al., 1989; Roth, 1989; Erba, 1992; Erba et al., 1992; Watkins et al., 2005; Hardas and Mutterlose, 2007). In lower fertility, oligotrophic surface water conditions, *Watznaueria* tends to dominate nannofossil populations (Roth and Krumback, 1986; Erba et al., 1992; Williams and Bralower, 1995; Herrle, 2002, 2003; Watkins et al., 2005; Hardas and Mutterlose, 2007).

Calcareous nannofloral paleoecology from the southern and central Western Interior Seaway is discussed in greater detail in Corbett and Watkins (2013), but a summary of observations from across Texas is presented here. At Lozier Canyon (Fig. 6a) the relative abundance of *Watznaueria* ranges from ~50–75% through the upper Cenomanian lower Eagle Ford and the middle Turonian unnamed member of the upper Eagle Ford. This suggests that the nannofossil recovery has been strongly affected by dissolution because *Biscutum* and *Zeugrhabdotus* make up less than 10% of the population through much of the section. As a result of this diagenetic overprinting, the data likely do not reflect the original death assemblage, and as a result TOC does not correspond to nannofossil paleoproductivity indicators. Preservation is better in the Fasken A #1-H and ACC #1 cores and can be compared with trends in planktic and benthic foraminifer abundance and TOC.

Watznaueria remains below 50% through most of the Eagle Ford in the ACC (Fig. 6b) and Fasken (Fig. 6c) cores, indicating the nannofossil abundances better reflect the original death assemblage. Populations preceding and following OAE2 are comprised of nearly 25–40% *Biscutum*. The abundance of *Biscutum* decreases to 10% or less through OAE2 in the Fasken core. Bio-chemostratigraphic interpretations reveal the interval spanning OAE2 to be missing from the ACC core and Bouldin Creek outcrops (Figs. 4B and 5B). No clear pattern in the abundance of *Zeugrhabdotus* is observed, though a small peak (~18%) is present in the uppermost Cenomanian of the Fasken core.

5. Discussion

5.1. Affinity with the Western Interior and oceanographic fronts

For the purposes of this study, we define an affinity to the Western Interior as rocks containing the following criteria: 1) peak TOC before the OAE2 interval; 2) foraminiferal faunal trends similar to those at Rock Canyon (e.g., "Benthonic Zone," "*Heterohelix* shift," HO of *Rotalipora* and *Globigerinelloides bentonensis* at or just after the onset of OAE2); and 3) lithologic transition similar to the Hartland–Bridge Creek (i.e., dark

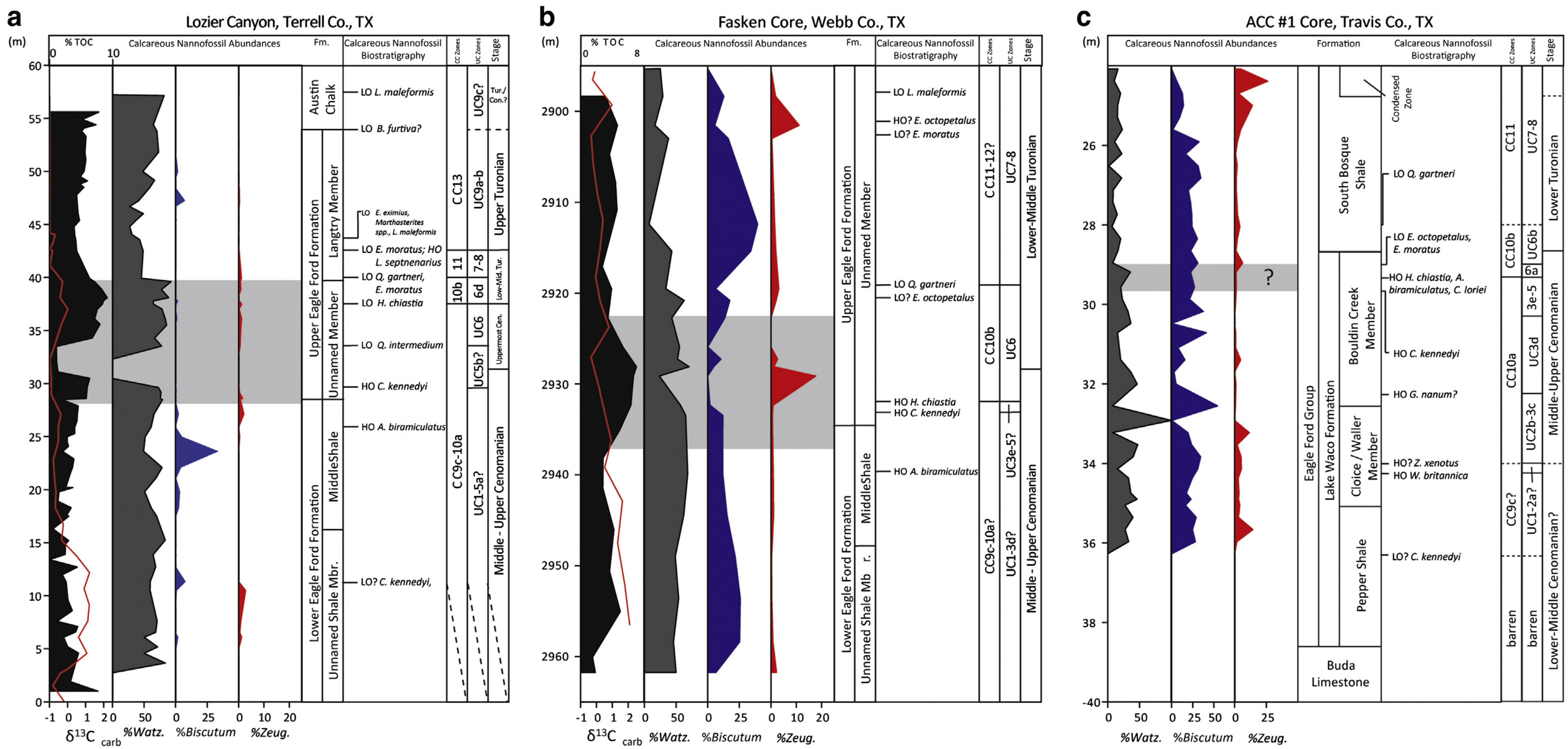

Fig. 6. Nannoplankton assemblage data from the Lozier Canyon outcrops in Terrell County (a), Fasken A #1H Core in Webb County (b), and ACC #1 Core in Travis County, 11 miles SE of the Bouldin Creek outcrop (c). Data include %*Watznaueria* spp., %*Biscutum* spp., and %*Zeugrhabdotus* spp., as well as the location of primary and secondary nannofossil data. The relative abundance of *Watznaueria* spp. is very high at the Lozier locality suggesting that nannofossil assemblages have been altered by diagenesis. Bulk carbonate isotope data ($\delta^{13}C_{carb}$) highlighted in black fill; weight percent total organic carbon (wt.% TOC) shown with red line. Gray bars show location of OAE2. (For interpretation of the references to color in this figure legend, the reader is referred to the web version of this article.)
Biostratigraphic data from Corbett et al. (2014).

gray organic rich shale overlain by light gray shale and limestones). All of our sites meet the TOC criteria, but only the platform sites meet the others.

The sites on the platform, including Frush and Eicher's (1975) Big Bend localities, show a lack of benthics before OAE2 and an obvious increase coincident with the onset of the anoxic event. Based on the well-documented structure of the OAE2 positive carbon isotope excursion, the last occurrence of *Rotalipora* at Lozier Canyon is earlier than at Rock Canyon. This south to north diachroneity was first noted in Big Bend by Frush and Eicher (1975) and has been interpreted to represent the south to north incursion of an oxygen minimum zone (OMZ) into the seaway (Leckie et al., 1998). Trends in biserial planktic foraminifera follow different patterns at each site, and while Lozier records a "*Heterohelix* shift" as observed at Rock Canyon and elsewhere in the Western Interior (Leckie et al., 1998), it is difficult to label this trend at the other Texas sites. Lithologically, Lozier Canyon and Big Bend also bear a strong resemblance to the Hartland Shale and Bridge Creek Limestone, which includes a limestone bed at Lozier Canyon at the base of the Middle Shale Mbr. corresponding to the onset of OAE2, the extinction of *Rotalipora*, and the beginning of the "benthonic zone," just like Bed 63 at Rock Canyon and HL1 in Kansas (Cobban and Scott, 1972; Hattin, 1975; Eicher and Diner, 1985; Elder and Kirkland, 1985).

The Fasken contains very few biserial planktics throughout, which is indicative of its deeper water, more open-marine location; Cenomanian–Turonian *Heterohelix* is generally associated with marginal environments and epeiric seas (Leckie, 1987; Leckie et al., 1998). Likewise, it has far more keeled planktic foraminifera, which tend to live deeper in the water column and are therefore also indicative of an open ocean setting (Ando et al., 2010).

Because sites on the Comanche Platform, especially the western platform, are very similar to the Western Interior, while the Fasken Core, to the southeast of the platform and in deeper water, bears no similarity to the Western Interior except for TOC trends, we conclude that the transition between the Western Interior Sea and the open ocean occurs at the edge of the Comanche Platform. But what controls organic carbon production, why is it the only similarity between the Fasken Core and the other sites, and why is it different from the global trend?

5.2. TOC trends, oxygenation, and productivity

The ratio of planktic to benthic foraminifera (P/B ratio, or %planktic to total foraminifera) is commonly used as a qualitative proxy for sea level and proximity to shore (e.g., Murray, 1976; Gibson, 1989; Hayward, 1990; Van der Zwaan et al., 1990; Leckie and Olson, 2003). However, in environments prone to dysoxia the P/B ratio is also a useful proxy for bottom water oxygenation (Van Hinsbergen et al., 2005). Proportions of major morpho-groups of planktic foraminifera are also useful proxies for bottom water or water column oxygenation, including biserial (*Heterohelix*, a generalist surface-dwelling genus that dominated stressed environments where other taxa do poorly), trochospiral (large, inflated thermocline to surface dwelling genera that include *Hedbergella*, *Whiteinella*, and *Archaeoglobigerina*), and keeled taxa (*Rotalipora*, *Praeglobotruncana*, *Dicarinella*, and *Marginotruncana*; genera that generally lived at deeper thermocline depths and/or normal marine environments), and the relative proportion of infaunal, typically low-oxygen tolerant benthic taxa (*Neobulimina*, especially, and other buliminids and rectilinear taxa) vs. epifaunal benthic taxa (*Gavelinella*, *Planulina*, *Lingulogavelinella*, and related trochospirally-coiled genera). Numerous studies have documented the usefulness of these foraminiferal groups for paleoceanographic interpretations across the Western Interior (e.g., Eicher and Diner, 1985; Leckie, 1985; Leckie et al., 1991; Fisher et al., 1994; Leckie et al., 1998; Caron et al., 2006).

Calcareous nannoplankton assemblages indicate that late Cenomanian surface water fertility through the high TOC intervals was comparable between the Fasken core and the Cloice Member (equivalent to the Middle Shale, Fig. 3) of the Eagle Ford in the ACC core. Higher abundances of *Biscutum* during intervals of high TOC suggest that elevated productivity in the photic zone led to an increased flux of organic matter into bottom waters and anoxia. Decreases in TOC and nannoplankton productivity indicators track each other. Slatt et al. (2012) show that the lower Eagle Ford is dominated by Type II kerogen, which indicates a marine source, further suggesting that the high TOC in the lower Eagle Ford is due to enhanced production.

The benthic foraminifera of the lower Eagle Ford agree with this interpretation, as do the planktics, although their signal is more complicated. The assemblages at Lozier Canyon (Fig. 5A) are initially dominated by biserial opportunist planktic foraminifera until trochospiral surface dwellers increase in abundance; deeper-dwelling keeled planktics remain rare, suggesting normal salinity but relatively shallow water (see below). In fact, biserials track TOC fairly closely at Lozier, while inoceramid abundance is roughly inversely related to biserial abundance. At Rock Canyon, Caron et al. (2006) recorded higher abundances of inoceramids when TOC is elevated but not at peak; a similar relationship is observed Lozier Canyon, with higher abundances of inoceramids at the transitions to rising and falling TOC levels. Bouldin Creek (Fig. 5B) has a fairly diverse, healthy planktic assemblage with a relatively diverse assemblage of keeled taxa and almost no biserials, even in the lower Eagle Ford where TOC is highest. Proximity to the shallow San Marcos Arch may have resulted in better mixing and a more oxic water column at Bouldin Creek. At Lozier Canyon, benthic foraminifera are generally anti-correlated to TOC (Fig. 7a). During the highest TOC intervals, benthic foraminifera are nearly absent. As TOC decreases, benthic foraminifera increase, initially just the low oxygen tolerant infaunal taxa (e.g., *Neobulimina albertensis*). The persistence of low-oxygen taxa when TOC is at or near zero, even as benthic foraminifera are more abundant and fairly diverse, suggests the persistence low-oxygen conditions even as anoxia abated. At Bouldin Creek, this only partially holds true (Fig. 7b). While benthics are absent in the highest TOC intervals, moderate TOC in the early Turonian coincides with high benthic values. In this case, clearly dysoxia did not prevent foraminifera from colonizing the area, perhaps reflecting decadal- to semi-annual variability not resolved in our data.

Recently published data from a Shell core drilled to the east of Lozier Canyon in the Maverick Basin support the interpretation of anoxia. Eldrett et al. (2014) show an enrichment of redox-sensitive trace elements, including Mo, U, V, Cu, and Ni, in the Lower Eagle, coincident with an interval of enriched TOC prior to OAE2, and declining to near zero during the anoxic event, suggesting anoxia in the Lower Eagle Ford and oxic conditions during OAE2.

The relationship between benthic foraminifera and carbon isotopes should also be noted. At Lozier, as elsewhere (Fig. 4), the positive carbon isotope excursion begins prior to the prominent limestone bed at the base of the Scott Ranch Member (equivalent to Bed 63 at Rock Canyon). At both Rock Canyon and Lozier Canyon, this precursor enrichment coincides with a slight increase in benthic foraminifera prior to the widespread "benthonic zone" at the onset of OAE2 (Elderbak et al., in this volume). The benthonic zone is weakly developed at the Lozier section, but still present.

Benthic foraminifera in the Fasken occur as isolated peaks, rather than a broad high mirroring TOC values. These trends are not artifacts of preservation; the peaks show clear trends of changing abundance in the samples before and after the acme, and the core contains abundant and occasionally well-preserved planktic foraminifera in samples with and without benthics. However, it seems highly unlikely that an epifaunal assemblage reminiscent of relatively shallow, oxic bottom waters would be in situ on an upper slope with high TOC laminated black shale. We believe that these peaks in benthic abundance are due to downslope transport from a much shallower, better oxygenated location. Although there is not a concomitant influx of *Heterohelix* with the epifaunal benthics, the presence of quartz grains in some samples, which roughly correspond to benthic peaks, supports the interpretation of displaced benthic foraminifera.

Please cite this article as: Lowery, C.M., et al., Foraminiferal and nannofossil paleoecology and paleoceanography of the Cenomanian–Turonian Eagle Ford Shale of southern Texas, Palaeogeogr. Palaeoclimatol. Palaeoecol. (2014), http://dx.doi.org/10.1016/j.palaeo.2014.07.025

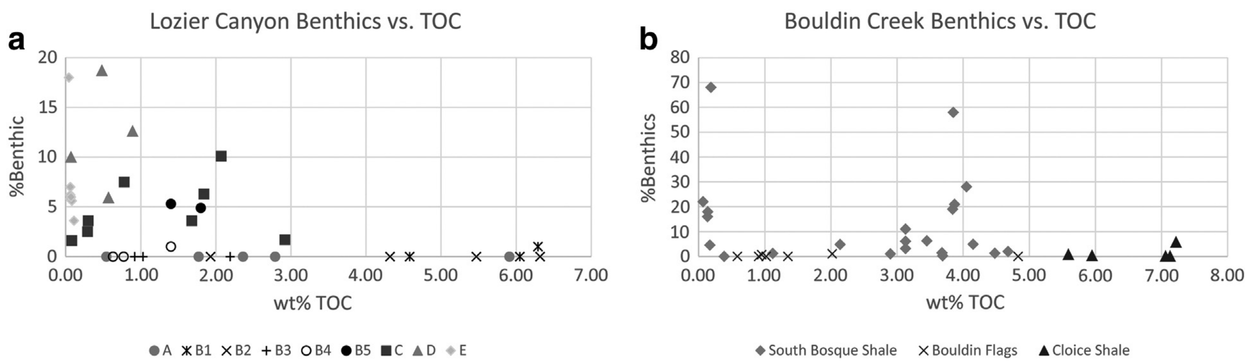

Fig. 7. Benthic foraminifera abundance vs. TOC cross plots for Lozier Canyon (a) and Bouldin Creek (b). Lozier Canyon is broken up by organic-facies (see Donovan et al., 2012 for detailed discussion): Facies A is lower Lozier Canyon Member, and which is totally barren of foraminifera (in this case, TOC-driven oxygen levels are not the limiting factor for foraminifer abundance); Facies B1 and B2 are the high TOC interval of the upper Lozier Canyon Member; Facies B3, B4, and B5 correspond to the Antonio Creek Member and are transitional from moderately high TOC (B3) to low TOC (B5); Facies C corresponds to the Scott Ranch Member (which corresponds to OAE2); Facies D and E correspond to the lower and upper Langtry Member. Bouldin Creek data is divided by members.

It seems likely that surface water productivity is driving organic matter preservation, which is controlling bottom water oxygenation, which in turn is driving benthic foraminiferal abundance and diversity. Long-term change in surface water productivity, we believe, is driven by changes in sea level. We hypothesize that the bathymetry-restricted flow into the WIS from the Gulf of Mexico facilitated bathymetry-induced upwelling of nutrients on and around the Comanche Platform. Wind-driven surface flow over the Stewart City Reef Trend would have brought more nutrients onto the platform, until eventually sea level rose high enough that surface flow would have less and less interaction with bathymetric features, and so upwelling (and productivity/OM content/anoxia) decreased gradually as sea level rose through the late Cenomanian. Alternatively, nutrients may have been supplied by runoff from the Ouachita Highlands to the northeast at this time (Sohl et al., 1991). We reject this hypothesis because it doesn't explain why TOC decreased as sea level increased, and moreover, we would expect to see an increase in weathering-derived nutrient flux, rather than the observed decrease, with the onset of OAE2 (Jenkyns, 2010).

The area of the Eagle Ford play (Fig. 1) is roughly parallel to shelf structure of the southern and eastern Comanche Platform, as might be expected if surface-flow over the buried older reef trends is driving upwelling. We suggest that the margin of the Comanche Platform was a localized upwelling cell that facilitated the production and burial of organic matter responsible for the Eagle Ford play today.

TOC enrichment in the Western Interior, on the other hand, is likely driven by enhanced preservation caused by restriction and stratification (e.g., Arthur and Sageman, 2005). While TOC trends in Texas and the Western Interior may appear to be unrelated events that coincidentally move in parallel, we suggest that the observed changes are related by a common driver: sea level rise. In Texas, late Cenomanian sea level slowly rose, reducing the effect of surface currents and bathymetry-induced upwelling. Likewise, in the Western Interior, late Cenomanian sea level rise brought increased communication with the open ocean and decreased stratification, eventually culminating in a dramatic increase in normal marine taxa and benthic foraminifera (Benthonic Zone), temporarily ventilating the water column (Leckie, 1985; Elderbak et al., in this volume).

5.3. Sea level variability/sequence stratigraphy

Sea level trends through the Cretaceous are well-known, and have been studied in Texas for over a century (Hill, 1887a,b). Sloss (1963) defined the 1st–3rd order sequences of the region, including the 3rd-order Eagle Fordian sequence. More recent work has further refined local sequence interpretations, as Donovan et al. (2012) described four 4th-order cycles in the Eagle Ford at Lozier Canyon. Planktic and benthic foraminiferal population trends, as well as sedimentary particles (dolomite rhombs, glauconite grains, macrofossil debris, etc.) record sea level changes across the Eagle Ford and serve to augment Donovan and colleagues' conclusions.

Above the disconformity at the top of the lower Cenomanian Buda Limestone, the Lozier Canyon Member records relatively low sea level. This is suggested by the occurrence of stacked hummocks and wave ripples (Donovan et al., 2012), as well as authigenic dolomite rhombs in the base of the member. The formation of these evaporite minerals indicates relatively shallow water depths and hypersalinity in west Texas during basal Eagle Ford time. High evaporation is to be expected in the subtropics during the hottest interval of the Cretaceous, but to explain even local hypersalinity that was strong enough to form evaporites, the Comanche Platform must have been fairly shallow and restricted. The Aptian and Albian reef buildups of the Stewart City Reef Trend probably served as a barrier to communication with surrounding normal marine waters of the Tethys and the brackish waters of the WIS. As sea level rose during the late Cenomanian, these conditions abated, and gave way to the high productivity conditions described above.

There is no microfossil evidence for the sequence boundary between the Lozier Canyon Member and the Antonio Creek Member. The slight increase in the percentage of benthic foraminifera beginning above the base of the Antonio Creek Member is presumably caused by improving conditions caused by rising sea level as evidenced from sedimentological features (Donovan et al., 2012). Similarly, there is no evidence for a sequence boundary between the Antonio Creek and Scott Ranch Members. Indeed, this level, equivalent to Bed 63 at Rock Canyon in Colorado and Bed HL-1 in Kansas, is conformable and is generally agreed to represent a isochronous flooding surface deposited as sea level rose rapidly and pelagic carbonate sedimentation began (e.g., Hattin, 1975; Elder et al., 1994; Tibert et al., 2003; Meyers and Sageman, 2004,; Arthur and Sageman, 2005).

The end of the OAE2 carbon-isotope excursion is truncated by a sequence boundary at Lozier Canyon. At Bouldin Creek, on the shallow San Marcos Arch, several nannofossil bioevents are condensed within a meter or less and the entire *Whiteinella archaeocretacea* Zone and OAE2 carbon isotope excursion are missing. The *W. archaeocretacea* Zone is also severely truncated at Hot Springs on the western margin of the platform (Frush and Eicher, 1975). This sequence boundary marks the beginning of the Langtry Member (equivalent to the South Bosque in the Austin area), where foraminiferal assemblages show a 4th-order T–R cycle with a decrease in benthic foraminifera toward a maximum flooding surface roughly halfway through the member (indicated by a nadir in %benthics and %*Heterohelix*) and then increasing toward a second sequence boundary at the top of the Eagle Ford.

The Langtry Member/South Bosque Member records shallower water depths toward the end of the Eagle Ford Cycle as evidenced by the increase in %benthic foraminifera, benthic macrofossils (inoceramids

Please cite this article as: Lowery, C.M., et al., Foraminiferal and nannofossil paleoecology and paleoceanography of the Cenomanian–Turonian Eagle Ford Shale of southern Texas, Palaeogeogr. Palaeoclimatol. Palaeoecol. (2014), http://dx.doi.org/10.1016/j.palaeo.2014.07.025

and echinoids), and return to hummocky bedforms. The end of the Eagle Ford Cycle is evident in a large late middle Turonian sea level fall that is equivalent to the Codell Sandstone Member of the Carlile Shale in southern Colorado, Kansas, and New Mexico, and represented as a major unconformity further north in the WIS (Hattin, 1975; Haq et al., 1987; Laferriere, 1987; Kauffman and Caldwell, 1993; Hancock and Walaszczyk, 2004). This sea level fall includes an erosional surface at Bouldin Creek and perhaps Lozier Canyon as well, although the data here are equivocal and it could be a lowstand without any erosion. The unconformity is characterized by acmes in %benthic and %biserial planktics, and gaps between nannofossil zones CC11 and CC13. This sequence boundary is immediately overlain by a thin (<1 m) transgressive lag deposit at both locations characterized by a sharp decrease in %benthics and %biserials, and the sudden appearance of glauconite at Bouldin Creek. In the Austin area, this event has been well documented as a "Rubble Zone" at the base of the Austin Chalk, filled with fish debris, glauconite, and phosphate nodules (e.g., Stephenson, 1929; Jiang, 1989; Lundquist, 2000). Some samples in this interval also contain reworked early Turonian taxa (e.g., *Eprolithus octopetalus*). The "Rubble Zone" has traditionally been mapped as part of the basal Atco Member of the Austin Chalk, with the unconformity as the Eagle Ford–Austin boundary. This interval is equivalent to the transgressive upper Turonian Juana Lopez Calcarenite Member of the Carlile Shale, a similar fossiliferous transgressive lag found in some locations in the WIS (particularly the southern WIS) between the Codell and the Fort Hays Member of the Niobrara Formation.

6. Conclusions

1. The Cenomanian–Turonian strata of the Comanche Platform is similar to the southern Western Interior Seaway (WIS), repeating paleoecological, geochemical, and lithologic patterns well known from the center of the seaway. The Eagle Ford Shale represents a 3rd-order transgressive–regressive sequence that is equivalent to the Greenhorn Cycle in the U.S. Western Interior Basin.
2. The Lozier Canyon and Bouldin Creek outcrop sections of the Eagle Ford on the Comanche Platform bear strong resemblance to sections of the Greenhorn and Carlile formations in the southern WIS based on planktic and benthic foraminiferal trends, including the "Benthonic Zone" at the onset of OAE2 and the "*Heterohelix* shift" during OAE2, dominance of the infaunal benthic foraminifer *Neobulimina albertensis*, and nannofossil assemblages. The Swift Fasken core, located on the South Texas submarine platform, records a deeper, more oceanic setting based on greater abundances of keeled planktic foraminifera, low abundances of *Heterohelix*, and abundances of radiolarians, particularly in the lower Eagle Ford.
3. Organic matter content in the lower Eagle Ford was driven by elevated primary productivity. A local, bathymetrically-induced upwelling cell developed off the southeastern flank of the Comanche Platform, along the South Texas submarine plateau, between the Albian Stuart City (Edwards) and Aptian Sligo shelf margin trends.
4. Total organic carbon (TOC) values, nannofossil assemblages, and radiolarian abundances all suggest that peak productivity occurred before the onset of Oceanic Anoxic Event 2 (OAE2), as recorded in the lower Eagle Ford. Productivity waned with rising sea level during the latest Cenomanian as the upwelling cell weakened and/or nutrients became increasingly sequestered in coastal wetlands and estuaries. OAE2 is associated with improved circulation between the Comanche Platform and the Western Interior Seaway, and perhaps incursion of an oxygen minimum zone from the Gulf of Mexico.
5. Bottom water oxygenation is correlated to TOC, and benthic foraminifera are very rare or absent where TOC is elevated. The OAE2 interval was associated with improved benthic oxygenation, but the presence of pyrite and dominance of infaunal *Neobulimina* at the Lozier section suggest the persistence of dysoxia at the seafloor and euxinic conditions within the sediments. The post-OAE2 interval at Lozier is marked by improved benthic oxygenation as indicated by greater abundances and diversity of benthic foraminifera and macrofossils.
6. The thickness variability of the Eagle Ford on and adjacent to the Comanche Platform is driven entirely by paleo-water depth and submarine erosion. Shallow sites near the rimming reef buildups or the San Marcos Arch are thinned, due both to lower accommodation and truncation due to relatively shallower water and submarine erosion. Deeper sites off the margins of the platform appear to be conformable and are therefore expanded. It is likely that the western slope sites are also expanded due to siliciclastic input from the adjacent tectonic uplift.

Acknowledgements

We gratefully acknowledge BP's North American Gas management for funding and supporting this project, as well as Art Donovan and Scott Staerker for their technical contributions and many discussions on the Eagle Ford. We are also indebted to Mike and Andrea Scott and Billy Foster for allowing us access to their land, and Swift Energy for access to their Fasken A 1H core. We are also very thankful for the assistance of Stephen Ruppel and James Donnelly and the permission of the Bureau of Economic Geology at the University of Texas at Austin for sampling of the ACC #1 core. We sincerely thank Richard Denne and Tim Bralower for their constructive reviews, and Tony Gary for his guidance as editor. We thank David Finkelstein of the UMass Isotope Geochemistry Lab for his invaluable assistance, Serena Dameron for her assistance with sample prep, and Lindsey Victoria for her assistance with the manuscript.

References

Ando, A., Huber, B.T., MacLeod, K.G., 2010. Depth–habitat reorganization of planktonic foraminifera across the Albian/Cenomanian boundary. Paleobiology 36, 357–373. http://dx.doi.org/10.1666/09027.1.

Arthur, M.A., Sageman, B.B., 2005. Sea level control on source rock development: perspectives from the Holocene Black Sea, the mid-Cretaceous Western Interior Basin of North America, and the Late Devonian Appalachian Basin. In: Harris, N.B. (Ed.), The Deposition of Organic Carbon-rich Sediments: Models, Mechanisms and Consequences. Society for Sedimentary Geology, Tulsa, pp. 35–59.

Arthur, M.A., Zachos, J.C., Jones, D.S., 1987. Primary productivity and the Cretaceous/Tertiary boundary event in the oceans. Cretaceous Res. 8, 43–45.

Arthur, M.A., Brumsack, H.J., Jenkyns, H.C., Schlanger, S.O., 1990. Stratigraphy, geochemistry, and paleoceanography of organic carbon-rich Cretaceous sequences. In: Ginsburg, R.N., Beaudoin, B. (Eds.), Cretaceous Resources, Events, and Rhythms. Kluwer, Dordrecht, pp. 75–119.

Barclay, R.S., McElwain, J.C., Sageman, B.B., 2010. Carbon sequestration activated by a volcanic CO_2 pulse during Oceanic Anoxic Event 2. Nat. Geosci. 3, 205–208.

Bralower, T.J., 1988. Calcareous nannofossil biostratigraphy and assemblages of the Cenomanian–Turonian boundary interval: implications for the origin and timing of oceanic anoxia. Paleoceanography 3, 275–316.

Bralower, T.J., Bergen, J.A., 1998. Cenomanian–Santonian calcareous nannofossil biostratigraphy of a transect of cores drilled across the Western Interior Seaway. In: Dean, W.E., Arthur, M.A. (Eds.), Stratigraphy and paleoenvironments of the Cretaceous Western Interior Seaway, USA. SEPM Concepts of Sedimentology and Paleontology. 6, pp. 59–77.

Burns, C.E., Bralower, T.J., 1998. Upper Cretaceous nannofossil assemblages across the Western Interior Seaway: implications for the origins of lithologic cycles in the Greenhorn and Niobrara Formations. In: Berggren, W.A., Kent, D.V., Aubry, M.-P., Harbendol, J. (Eds.), Geochronology times scales and global stratigraphic correlation. SEPM Special Publication. 54, pp. 35–58.

Caron, M., 1985. Cretaceous planktic foraminifera. In: Bolli, H.M., Saunders, J.B., Perch-Nielsen, K. (Eds.), Plankton Stratigraphy. Cambridge University Press, pp. 17–86.

Caron, M., Dall'Agnolo, S., Accarie, H., Barrera, E., Kauffman, E.G., Amédro, D., Robaszynski, F., 2006. High-resolution stratigraphy of the Cenomanian–Turonian boundary interval at Pueblo (USA) and Wadi Bahloul (Tunisia): stable isotope and bio-events correlation. Géobios 39, 171–200.

Cobban, W.A., Scott, G.R., 1972. Stratigraphy and ammonite fauna of the Graneros Shale and Greenhorn Limestone near Pueblo, Colorado. Washington, D.C. U.S. Geological Survey Professional Paper. 645 (108 p.).

Cobban, W.A., Hook, S.C., McKinney, K.C., 2008. Upper Cretaceous molluscan record along a transect from Virden, New Mexico, to Del Rio, Texas. N. M. Geol. 30, 75–92.

Corbett, M.J., Watkins, D.K., 2013. Calcareous nannofossil paleoecology of the mid-Cretaceous Western Interior Seaway and evidence of oligotrophic surface waters during OAE2. Palaeogeogr. Palaeoclimatol. Palaeoecol. 392, 510–523.

Corbett, M.J., Watkins, D.K., Popspichal, J.J., 2014. A quantitative analysis of calcareous nannofossil bioevents of the Late Cretaceous (Late Cenomanian–Coniacian) Western

Interior Seaway and their reliability in established zonation schemes. Mar. Micropaleontol. 109, 30–45.

Denne, R.A., Hinote, R.E., Breyer, J.A., Kosanke, T.H., Lees, J.A., Engelhardt-Moore, N., Spaw, J.M., Tur, N., 2014. The Cenomanian–Turonian Eagle Ford Group of South Texas: insights on timing and paleoceanographic conditions from geochemistry and micropaleontologic analyses. Palaeogeogr. Palaeoclimatol. Palaeoecol. http://dx.doi.org/10.1016/j.palaeo.2014.05.029.

Desmares, D., Grosheny, D., Beaudoin, B., Gardin, S., Gauthier-Lafaye, F., 2007. High-resolution stratigraphic record constrained by volcanic ash beds at the Cenomanian–Turonian boundary in the Western Interior Basin, USA. Cretaceous Res. 28, 561–582.

Donovan, A.D., Staerker, T.S., 2010. Sequence stratigraphy of the Eagle Ford (Boquillas) formation in the subsurface of south Texas and the outcrops of west Texas. Gulf Coast Assoc. Geol. Soc. Trans. 60, 861–899.

Donovan, A.D., Staerker, T.S., Pramudito, A., Li, W., Corbett, M.J., Lowery, C.M. Miceli, Romero, A., Gardner, R.D., 2012. The Eagle Ford outcrops of west Texas: a laboratory for understanding heterogeneities within unconventional mudstone reservoirs. Gulf Coast Assoc. Geol. Soc. J. 1, 162–185.

Eicher, D.L., 1965. Foraminifera and biostratigraphy of the Graneros Shale. J. Paleontol. 39, 875–909.

Eicher, D.L., 1966. Foraminifera of the Cretaceous Carlile Shale of Colorado. Cushman Found. Foram. Res. Contrib. 17, 16–31.

Eicher, D.L., 1969. In: Bronnimann, P., Renz, H.H. (Eds.), Cenomanian Turonian planktonic foraminifera from the Western Interior of the United StatesProceedings of the First International Conference on Planktonic Microfossils. 2. E.J. Brill, Leiden, pp. 163–174.

Eicher, D.L., Diner, R., 1985. Foraminifera as indicators of water mass in the Cretaceous Greenhorn Sea, Western Interior. In: Pratt, L., Kauffman, E.G., Zelt, F.B. (Eds.), Fine-grained deposits and biofacies of the Cretaceous Western Interior Seaway: evidence of cyclic depositional processes. SEPM Annual Mid-year Meeting, Field Trip No. 4, pp. 122–134.

Eicher, D.L., Diner, R., 1989. Origin of the Cretaceous Bridge Creek cycles in the Western Interior, United States. Palaeogeogr. Palaeoclimatol. Palaeoecol. 74, 127–146.

Eicher, D.L., Worstell, P., 1970. Cenomanian and Turonian foraminifera from the Great Plains, United States. Micropaleontology 16, 269–324.

Elder, W.P., 1985. Biotic patterns across the Cenomanian–Turonian boundary near Pueblo, Colorado. In: Pratt, L., Kauffman, E.G., Zelt, F.B. (Eds.), Fine-grained deposits and biofacies of the Cretaceous Western Interior Seaway: evidence of cyclic depositional processes. SEPM Annual Mid-year Meeting, Field Trip No. 4, pp. 157–169.

Elder, W.P., 1989. Molluscan extinction patterns across the Cenomanian–Turonian stage boundary in the western interior of the United States. Paleobiology 15, 299–320.

Elder, W.P., 1991. Molluscan paleoecology and sedimentation patterns of the Cenomanian–Turonian extinction interval in the southern Colorado Plateau region. In: Nations, J.D., Eaton, J.G. (Eds.), Stratigraphy, depositional environments, and sedimentary tectonics of the Western Margin, Cretaceous Western Interior SeawaySpecial Paper. 260. Geological Society of America, Boulder, pp. 113–137.

Elder, W.P., Kirkland, J.I., 1985. Stratigraphy and depositional environments of the Bridge Creek Limestone Member of the Greenhorn Limestone at Rock Canyon Anticline near Pueblo, Colorado. In: Pratt, L., Kauffman, E.G., Zelt, F.B. (Eds.), Fine-grained deposits and biofacies of the Cretaceous Western Interior Seaway: evidence of cyclic depositional processes. SEPM Annual Mid-year Meeting, Field Trip No. 9, pp. 122–134.

Elder, W.P., Gustason, E.R., Sageman, B.B., 1994. Correlation of basinal carbonate cycles to nearshore parasequences in the Late Cretaceous Greenhorn seaway, Western Interior U.S.A. Geol. Soc. Am. Bull. 106, 892–902.

Elder, W.P., Kirkland, J.I., 1994. Cretaceous paleogeography of the southern Western Interior region. In: Caputo, M.V., Peterson, J.A., Franczyk (Eds.), Mesozoic System of the Rocky Mountain Region, U.S.A., Rocky Mountain Section, Society for Sedimentary Geology, pp. 415–440.

Elderbak, K., Leckie, R.M., Tibert, N.E., 2014. Paleoenvironmental and paleoceanographic changes across the Cenomanian–Turonian Boundary Event (Oceanic Anoxic Event 2) as indicated by foraminiferal assemblages from the eastern margin of the Cretaceous Western Interior Seaway. Palaeogeogr. Palaeoclimatol. Palaeoecol. (in this volume).

Eldrett, J.S., Minisini, D., Bergman, S.C., 2014. Decoupling of the carbon cycle during Oceanic Anoxic Event 2. Geology http://dx.doi.org/10.1130/G35520.1.

Eleson, J.W., Bralower, T.J., 2005. Evidence of changes in surface water temperature and productivity at the Cenomanian/Turonian Boundary. Micropaleontology 51, 319–322.

Erba, E., 1992. In: Lawson, R.L., Lancelot, Y. (Eds.), Middle Cretaceous nannofossils from the Western Pacific (ODP Left 129): evidence for paleoequatorial crossings. Proceedings of the Ocean Drilling Program Scientific Results. 129, pp. 189–201.

Erba, E., 2004. Calcareous nannofossils and Mesozoic oceanic anoxic events. Marine Micropaleontology 52, 85–106.

Erba, E., Castradori, G., Guasti, G., Ripepe, M., 1992. Calcareous nannofossils and Milankovitch cycles: the example of the Albian Gault Clay Formation (southern England). Palaeogeogr. Palaeoclimatol. Palaeoecol. 93, 47–69. http://dx.doi.org/10.1016/0031-0182(92)90183-6.

Erbacher, J., Thurow, J., 1997. Influence of oceanic anoxic events on the evolution of mid-Cretaceous radiolaria in the North Atlantic and western Tethys. Mar. Micropaleontol. 30, 139–158.

Erbacher, J., Thurow, J., Littke, R., 1996. Evolution patterns of radiolaria and organic matter variations: a new approach to identify sea-level changes in mid-Cretaceous pelagic environments. Geology 24, 499–502.

Fisher, C.G., Hay, W.W., Eicher, D.L., 1994. Oceanic front in the Greenhorn Sea (late middle through late Cenomanian). Paleoceanography 9, 879–892.

Friedrich, O., 2010. Benthic foraminifera and their role to decipher paleoenvironment during mid-Cretaceous Oceanic Anoxic Events — the "anoxic benthic foraminifera" paradox. Rev. Micropaléontol. 53, 175–192.

Friedrich, O., Erbacher, J., Mutterlose, J., 2006. Paleoenvironmental changes across the Cenomanian/Turonian boundary event (Oceanic Anoxic Event 2) as indicated by benthic foraminifera from the Demerara Rise (ODP Leg 207). Rev. Micropaléontol. 49, 121–139.

Friedrich, O., Norris, R.D., Erbacher, J., 2012. Evolution of Late Cretaceous oceans — a 55 m.y. record of Earth's temperature and carbon cycle. Geology 40, 107–110.

Frush, M.P., Eicher, D.L., 1975. Cenomanian and Turonian foraminifera and paleoenvironments in the Big Bend region of Texas and Mexico. In: Caldwell, W.G.E. (Ed.), The Cretaceous System in the Western Interior of North America. The Geological Society of Canada Special Paper. 13, pp. 277–301.

Gale, A.S., Smith, A.B., Monks, N.A.E., Young, J.A., Howard, A., Wray, D.S., Huggett, J.M., 2000. Marine biodiversity through the Late Cenomanian–Early Turonian: palaeoceanographic controls and sequence stratigraphy biases. J. Geol. Soc. 157, 745–757.

Gale, A.S., Kennedy, W.J., Voight, S., Walaszczyk, I., 2005. Stratigraphy of the Upper Cenomanian–Lower Turonian chalk succession at Eastbourne, Sussex, UK: ammonites, inoceramid bivalves, and stable carbon isotopes. Cretaceous Res. 26, 460–487.

Gale, A.S., Voigt, S., Sageman, B.B., Kennedy, W.J., 2008. Eustatic sea-level record for the Cenomanian (Late Cretaceous) — extension to the Western Interior Basin, USA. Geology 36, 859–862.

Geisen, M., Bollman, J., Herrle, J.O., Mutterlose, J., Young, J.R., 1999. Calibration of the random settling technique for calculation of absolute abundances of calcareous nannoplankton. Micropaleontology 45, 437–442.

Gibson, T.G., 1989. Planktonic: benthonic foraminiferal ratios: modern patterns and Tertiary applicability. Mar. Micropaleontol. 15, 29–52.

Gradstein, F.M., Ogg, J.G., Schmitz, M., Ogg, G., 2012. The Geologic Time Scale. Elsevier, Amsterdam, The Netherlands.

Hancock, J.M., Walaszczyk, I., 2004. Mid-Turonian to Coniacian changes of sea level around Dallas, Texas. Cretaceous Res. 25, 459–471.

Haq, B.V., Harbendol, J., Vail, P.R., 1987. Chronology of fluctuating sea levels since the Triassic (250 million years ago to present). Science 235, 1159–1167.

Hardas, P., Mutterlose, J., 2007. Calcareous nannofossil assemblages of Oceanic Anoxic Event 2 in the equatorial Atlantic: evidence of an eutrophication event. Mar. Micropaleontol. 66, 52–69.

Hattin, D.E., 1971. Widespread, synchronously deposited, burrow-mottled limestone beds in Greenhorn Limestone (Upper Cretaceous) of Kansas and central Colorado. AAPG Bull. 55, 412–431.

Hattin, D.E., 1975. Stratigraphy and depositional environment of Greenhorn Limestone (Upper Cretaceous) of Kansas. Kansas Geol. Surv. Bull. 209, 128.

Hayward, B.W., 1990. Use of foraminiferal data in analysis of Taranaki basin, New Zealand. J. Foramin. Res. 20, 71–83.

Hazzard, R.T., 1959. Measured section. In: Cannon, R.L., Hazzard, R.T., Young, A., Young, K.P. (Eds.), Geology of the Val Verde Basin. West Texas Geological Society Guidebook, Midland (November 5–8, 118 p.).

Hentz, T.F., Ruppel, S.C., 2010. Regional lithostratigraphy of the Eagle Ford Shale: Maverick Basin to East Texas Basin. Gulf Coast Assoc. Geol. Soc. Trans. 60, 325–337.

Herrle, J.O., 2002. Paleoceanographic and paleoclimatic implications on mid-Cretaceous black shale formation in the Vocontian Basin and the Atlantic: evidence from calcareous nannofossils and stable isotopes. Tübinger Mikropaläontologische Mitt. 27, 1–114.

Herrle, J.O., 2003. Reconstructing nitricline dynamics of mid-Cretaceous oceans; evidence from calcareous nannofossils from the Niveau Paquier black shale (SE France). Mar. Micropaleontol. 47, 307–321. http://dx.doi.org/10.1016/S0377-8398(02)00133-0.

Hill, R.T., 1887a. The topography and geology of the Cross Timbers and surrounding regions in northern Texas. Am. J. Sci. 33, 291–303 (3rd Series).

Hill, R.T., 1887b. The Texas section of the American Cretaceous. Am. J. Sci. 34, 287–309 (3rd Series).

Huber, B.T., Petrizzo, M.R., 2014. Evolution and taxonomic study of the Cretaceous planktic foraminiferal genus *Helvetoglobotruncana* Reiss, 1957. J. Foramin. Res. 44, 40–57.

Jarvis, I., Gale, A.S., Jenkyns, H.C., Pearce, M.A., 2006. Secular variation in Late Cretaceous carbon isotopes: a new $\delta^{13}C$ carbonate reference curve for the Cenomanian–Campanian (99.6–70.6 Ma). Geol. Mag. 143, 561–608.

Jarvis, I., Lignum, J.S., Gröcke, D.R., Jenkyns, H.C., Pearce, M.A., 2011. Black Shale deposition, atmospheric CO_2 drawdown, and cooling during the Cenomanian-Turonian Oceanic Anoxic Event. Paleoceanography 26, PA3201. http://dx.doi.org/10.1029/2010PA002081.

Jenkyns, H.C., 1980. Cretaceous anoxic events: from continents to oceans. J. Geol. Soc. 137, 171–188. http://dx.doi.org/10.1144/gsjgs.137.2.0171.

Jenkyns, H.C., 2010. Geochemistry of oceanic anoxic events. Geochem. Geophys. Geosyst. 11, 30.

Jiang, M.J., 1989. Biostratigraphy and Geochronology of the Eagle Ford Shale, Austin Chalk, and Lower Taylor Marl in Texas Based on Calcareous Nannofossils. Ph.D. dissertation Texas A&M University (496 p.).

Kaiho, K., Hasegawa, T., 1994. Cenomanian benthic foraminiferal extinctions and dysoxic events in the northwestern Pacific Ocean margin. Palaeogeogr. Palaeoclimatol. Palaeoecol. 111, 29–43.

Kauffman, E.G., 1977a. Geological and biological overview: Western Interior Cretaceous Basin. In: Kauffman, E.G (Ed.), Cretaceous facies, faunas and paleoenvironments across the Western Interior Basin. Mountain Geologist. 14, pp. 75–99.

Kauffman, E.G., 1977b. Upper Cretaceous cyclothems, biotas, and environments, Rock Canyon Anticline, Pueblo, Colorado. In: Kauffman, E.G (Ed.), Cretaceous facies, faunas, and paleoenvironments across the Western Interior Basin. Mountain Geologist. 14, pp. 129–152.

Kauffman, E.G., 1984. Paleobiogeography and evolutionary response dynamic in the Cretaceous Western Interior Seaway of North America. In: Westermann, G.E.G. (Ed.), Jurassic–Cretaceous biochronology and paleogeography of North America. Geological Association of Canada Special Paper. 27, pp. 273–306.

Kauffman, E.G., Caldwell, W.G.E., 1993. The Western Interior Basin in space and time. In: Kauffman, E.G., Caldwell, W.G.E. (Eds.), Evolution of the Western Interior Basin. Geological Association of Canada Special Paper. 39, pp. 1–30.

Kauffman, E.G., Pratt, L.M., 1985. A field guide to the stratigraphy, geochemistry, and depositional environments of the Kiowa–Skull Creek, Greenhorn, and Niobrara marine cycles in the Pueblo–Canon City Area, Colorado. In: Pratt, L.M., Kauffman, E.G., Zelt, F.B. (Eds.), Fine-grained Deposits and Biofacies of the Cretaceous Western Interior Seaway: Evidence of Cyclic Sedimentary Processes. Society of Economic Paleontologists and Mineralogists, Tulsa, pp. 250–276.

Kennedy, W.J., Walaszczyk, I., Cobban, W.A., 2005. The global boundary stratotype section and point for the base of the Turonian Stage of the Cretaceous: Pueblo, Colorado, U.S.A. Episodes 28, 93–104.

Laferriere, A.P., 1987. Cyclic sedimentation in the Fort Hays Limestone Member, Niobrara Formation (Upper Cretaceous) in northeastern New Mexico and southeastern Colorado. New Mexico Geological Society 38th Field Conference. Guidebook, Northeastern New Mexico, pp. 249–254.

Leckie, R.M., 1985. Foraminifera of the Cenomanian–Turonian boundary interval, Greenhorn Formation, Rock Canyon Anticline, Pueblo, Colorado. In: Pratt, L., Kauffman, E.G., Zelt, F.B. (Eds.), Fine-grained deposits and biofacies of the Cretaceous Western Interior Seaway: evidence of cyclic depositional processes. SEPM Annual Mid-year Meeting, Field Trip No. 4, pp. 139–149.

Leckie, R.M., 1987. Paleoecology of mid-Cretaceous planktonic foraminifera: a comparison of open ocean and epicontinental sea assemblages. Micropaleontology 33 (2), 164–176.

Leckie, R.M., Olson, H.C., 2003. Foraminifera as proxies for sea-level change on siliciclastic margins. In: Leckie, R.M., Olson, H.C. (Eds.), Micropaleontologic proxies for sea-level change and stratigraphic discontinuities. SEPM Special Publication No. 75, pp. 5–19.

Leckie, R.M., Schmidt, M., Finkelstein, D., Yuretich, R., 1991. Paleoceaographic and paleoclimatic interpretations of the Mancos Shale (Upper Cretaceous), Black Mesa Basin, Arizona. In: Nations, D., Eaton, J. (Eds.), Stratigraphy, depositional environments and sedimentary tectonics of the southwestern margin, Cretaceous Western Interior Seaway. Geological Society of America Special Paper. 260, pp. 139–152.

Leckie, R.M., Kirkland, J.I., Elder, W.P., 1997. Stratigraphic framework and correlation of a principal reference section of the Mancos Shale (Upper Cretaceous), Mesa Verde, Colorado. New Mexico Geological Society Guidebook, 48th field conference. Mesozoic Geology and Paleontology of the Four Corners Region, pp. 163–216.

Leckie, R.M., Yuretich, R.F., West, O.L.O., Finkelstein, D., Schmidt, M., 1998. Paleoceanography of the southwestern Western Interior Sea during the time of the Cenomanian–Turonian boundary (Late Cretaceous). In: Dean, W.E., Arthur, M.A. (Eds.), Stratigraphy and paleoenvironments of the Cretaceous Western Interior Seaway, U.S.A. SEPM Concepts in Sedimentology and Paleontology. 6, pp. 101–126.

Leckie, R.M., Bralower, T.J., Cashman, R., 2002. Oceanic anoxic events and plankton evolution: biotic response to tectonic forcing during the mid-Cretaceous. Paleoceanography 17. http://dx.doi.org/10.1029/2001PA000623.

Linnert, C., Mutterlose, Erbacher, J., 2010. Calcareous nannofossils of the Cenomanian/Turonian boundary interval from the Boreal Realm (Wunstorf, northwest Germany). Mar. Micropaleontol. 74, 38–58.

Linnert, C., Mutterlose, J., Herrle, J.O., 2011. Late Cretaceous (Cenomanian–Maastrichtian) calcareous nannofossils from Goban Spur (DSDP Sites 549). Palaeoclimatol. Palaeoecol. 299, 507–528.

Lock, B.E., Peschier, L., Whitcomb, N., 2010. The Eagle Ford (Boquillas Formation) of Val Verde County, Texas—a window on the South Texas play. Gulf Coast Assoc. Geol. Soc. Trans. 60, 419–434.

Lundquist, J.J., 2000. Foraminiferal Biostratigraphic and Paleoceanographic Analysis of the Eagle Ford, Austin, and Lower Taylor Groups (Middle Cenomanian through Lower Campanian) of Central Texas. University of Texas at Austin (Ph.D. dissertation, 545 p.).

Meyers, S.R., Sageman, B.B., 2004. Detection, quantification, and significance of hiatuses in pelagic and hemipelagic strata. Earth Planet. Sci. Lett. 224, 55–72.

Meyers, S., Sageman, B.B., Hinnov, L., 2001. Integrated quantitative stratigraphy of Cenomanian–Turonian Bridge Creek Limestone Member using evolutive harmonic analysis and stratigraphic modeling. J. Sediment. Res. 71, 628–644.

Meyers, S.R., Sageman, B.B., Lyons, T.W., 2005. Organic carbon burial rate and the molybdenum proxy: theoretical framework and application to Cenomanian–Turonian Oceanic Anoxic Event 2. Paleoceanography 20, PA2002. http://dx.doi.org/10.1029/2004PA001068.

Monteiro, F.M., Pancost, R.D., Ridgwell, A., Donnadieu, Y., 2012. Nutrients as the dominant control on the spread of anoxia and euxinia across the Cenomanian–Turonian ocean anoxic event (OAE2): model-data comparison. Paleoceanography 27, PA4209. http://dx.doi.org/10.1029/2012PA002351.

Murray, J.W., 1976. A method of determining proximity of marginal seas to an ocean. Mar. Geol. 22, 103–119.

Norris, R.D., Wilson, P.A., 1998. Low-latitude sea-surface temperatures for the mid-Cretaceous and the evolution of planktic foraminifera. Geology 26, 823–826.

Owens, J.D., Lyons, T.W., Li, X., MacLeod, K.G., Gordon, G., Kuypers, M.M.M., Anbar, A., Kuhnt, W., Severmann, S., 2012. Iron isotope and trace metal records of iron cycling in the proto-North Atlantic during the Cenomanian–Turonian Oceanic Anoxic Event (OAE-2). Paleoceanography 27, PA3223. http://dx.doi.org/10.1029/2012PA002328.

Paul, C.R.C., Lamolda, M.A., Mitchell, S.F., Vaziri, M.R., Gorostidi, A., Marshall, J.D., 1999. The Cenomanian–Turonian boundary at Eastbourne (Sussex, UK): a proposed European reference section. Palaeogeogr. Palaeoclimatol. Palaeoecol. 150, 83–121.

Pessagno, E., 1969. GSA Memoir 111, Upper Cretaceous Stratigraphy of the Western Gulf Coast Area of Mexico, Texas, and Arkansas (139 p.).

Petrizzo, M.R., Huber, B.T., Wilson, P.A., MacLeod, K.G., 2008. Late Albian paleoceanography of the western subtropical North Atlantic. Paleoceanography PA1213 http://dx.doi.org/10.1029/2007PA001517.

Pratt, L.M., 1985. Isotopic studies of organic matter and carbonate in rocks of the Greenhorn marine cycle. In: Pratt, L.M., Kauffman, E.G., Zelt, F.B. (Eds.), Fine-grained Deposits and Biofacies of the Cretaceous Western Interior Seaway: Evidence of Cyclic Sedimentary Processes. Society of Economic Paleontologists and Mineralogists, Tulsa, pp. 38–59.

Pratt, L.M., Threlkeld, C.N., 1984. Stratigraphic significance of $^{13}C/^{12}C$ ratios in mid-Cretaceous rocks of the Western Interior, U.S.A. In: Stott, D.F., Glass, D.J. (Eds.), The Mesozoic of Middle North America. Canadian Society of Petroleum Geologists Memoir. 9, pp. 305–312.

Pratt, L.M., Arthur, M.A., Dean, W.E., Scholle, P.A., 1993. In: Caldwell, W.G.E., Kauffman, E.G. (Eds.), Paleo-oceanographic cycles and events during the Late Cretaceous in the Western Interior seaway of North America. Evolution of the Western Interior Basin Geological Association of Canada Special Paper. 39, pp. 333–353.

Premoli-Silva, I., Sliter, W.V., 1999. Cretaceous paleoceanography: evidence from planktonic foraminiferal evolution. In: Barrera, E., Johnson, C. (Eds.), Evolution of the Cretaceous ocean–climate system. Geological Society of America Special Paper. 332, pp. 301–328.

Premoli-Silva, I., Erba, E., Tornaghi, M.E., 1989. Paleoenvironmental signals and changes in surface fertility in Mid Cretaceous C_{org}-rich pelagic of the Fucoid Marls (central Italy). Geobios 22, 225–236. http://dx.doi.org/10.1016/S0016-6995(89)80059-2.

Roth, P.H., 1981. Mid-Cretaceous calcareous nannoplankton from the central Pacific: implications for paleoceanography. Init. Rep. Deep Sea Drilling Proj. 62, 471–489.

Roth, P.H., 1986. In: Summerhays, C.P., Shackelton, N.J. (Eds.), Mesozoic paleoceanography of the North Atlantic Tethys oceans. Geological Society of America Special, Publication. 21, pp. 299–320.

Roth, P.H., 1989. Ocean circulation and calcareous nannoplankton evolution during the Jurassic and Cretaceous. Palaeogeogr. Palaeoclimatol. Palaeoecol. 74, 111–126. http://dx.doi.org/10.1016/0031-0182(89)90022-9.

Roth, P.H., Bowdler, J., 1981. Middle Cretaceous calcareous nannoplankton biogeography and oceanography of the Atlantic Ocean. In: Warme, J.E., Douglas, R.G., Winterer, E.L. (Eds.), The Deep Sea Drilling Project: a decade of progress. SEPM Special Publication. 32, pp. 517–546.

Roth, P.H., Krumback, K.R., 1986. Middle Cretaceous calcareous nannofossil biogeography and preservation in the Atlantic and Indian Oceans: implications for paleoceanography. Mar. Micropaleontol. 10, 235–266. http://dx.doi.org/10.1016/0377-8398(86)90031-9.

Sageman, B.B., 1985. High-resolution stratigraphy and paleobiology of the Hartland Shale Member: analysis of an oxygen-deficient epicontinental sea. In: Pratt, L.M., Kauffman, E.G., Zelt, F.B. (Eds.), Fine-grained deposits and biofacies of the Cretaceous Western Interior Seaway: evidence of cyclic sedimentary processes. SEPM Mid-year Annual Meeting, Field Trip No. 4, pp. 110–121.

Sageman, B.B., Arthur, M.A., 1994. Early Turonian paleogeographic/paleobathymetric map, Western Interior, US. In: Caputo, M., Peterson, J. (Eds.), Mesozoic systems of the Rocky Mountain region, U.S. Society of Economic Paleontologists and Mineralogists Special Publication, Rocky Mountain Section, pp. 457–470.

Sageman, B.B., Rich, J., Arthur, M.A., Dean, W.E., Savrda, C.E., Bralower, T.J., 1998. Multiple Milankovitch cycles in the Bridge Creek Limestone (Cenomanian–Turonian), Western Interior Basin. Concepts Sedimentol. Paleontol. 6, 153–171.

Sageman, B.B., Meyers, S.R., Arthur, M.A., 2006. Orbital time scale and new C-isotope record for Cenomanian–Turonian boundary stratotype. Geology 34, 125–128.

Savrda, C.E., Bottjer, D.J., 1993. Trace fossil assemblages in fine-grained strata of the Cretaceous western interior. In: Caldwell, W.G.E., Kauffman, E.G. (Eds.), Evolution of the Western Interior Basin. Geological Association of Canada Special Paper. 39, pp. 621–639.

Schlanger, S.O., Jenkyns, H.C., 1976. Cretaceous oceanic anoxic events: causes and consequences. Geol. Mijnb. 55, 179–184.

Schlanger, S.O., Arthur, M.A., Jenkyns, H.C., Scholle, P.A., 1987. The Cenomanian–Turonian Oceanic Anoxic Event I. Stratigraphy and distribution of organic carbon-rich beds and the marine δ C excursion. In: Brooks, J., Fleet, A.J. (Eds.), Marine petroleum source rocks. Geological Society Special Publication. 26, pp. 371–399.

Scholle, P.A., Arthur, M.A., 1980. Carbon isotope fluctuations in Cretaceous pelagic limestones: potential stratigraphic and petroleum exploration tool. AAPG Bull. 64, 67–87.

Slatt, R.M., O'Brien, N.R., Romero, A.M., Rodriguez, H.H., 2012. Eagle Ford condensed section and its oil and gas storage and flow potential. AAPG Search and Discovery Article 80245.

Sloss, L., 1963. Sequences of the cratonic interior of North America. Geol. Soc. Am. Bull. 74, 93–114.

Smith, C.C., 1981. Calcareous nannoplankton and stratigraphy of late Turonian, Coniacian, and early Santonian age of the Eagle Ford and Austin groups of Texas. U.S. Geological Society Professional Paper 1075 (96 p.).

Snow, L.J., Duncan, R.A., Bralower, T.J., 2005. Trace element abundances in the Rock Canyon Anticline, Pueblo, Colorado, marine sedimentary section and their relationship to Caribbean plateau construction and Oxygen Anoxic Event 2. Paleoceanography 20, PA3005. http://dx.doi.org/10.1029/2004PA001093.

Sohl, N.F., Martinez, E.R., Salmerón-Ureña, P., Soto-Jaramillo, F., 1991. Upper Cretaceous. In: Salvador, A. (Ed.), The Geology of North America Volume J: Gulf of Mexico Basin. Geological Society of America, Boulder, CO.

Stephenson, 1929. Unconformities in the Upper Cretaceous series of Texas. AAPG Bull. 13, 1323–1334.

Tantawy, A.A., 2008. Calcareous nannofossil biostratigraphy and paleoecology of the Cenomanian–Turonian transition in the central desert of Egypt. Mar. Micropaleontol. 47, 323–356.

Thierstein, H.R., 1981. Late Cretaceous nannoplankton and the change at the Cretaceous–Tertiary boundary. In: Douglas, R.C., Winterer, E.L. (Eds.), The Deep Sea Drilling Project: a decade of progress. SEPM Special Publication. 32, pp. 355–394.

Tibert, N.E., Leckie, R.M., Eaton, J.G., Kirkland, J.I., Colin, J.P., Leithold, E.L., McCormic, M., 2003. Recognition of relative sea level change in Upper Cretaceous coal-bearing strata: a paleoecological approach using agglutined foraminifera and ostracodes to detect key stratigraphic surfaces. In: Olson, H., Leckie, R.M. (Eds.), Microfossils as a proxy for sea level changes and stratigraphic discontinuities. Society for Sedimentary Geology (SEPM) Special Publication, pp. 263–299.

Tsikos, H., Jenkyns, H., Walsworth-Bell, B., Petrizzo, M.R., Forster, A., Kolonic, S., Erba, E., Premoli Silva, I., Baas, M., Wagner, T., Sinninghe Damsté, J.S., 2004. Carbon-isotope stratigraphy recorded by the Cenomanian–Turonian oceanic anoxic event: correlation and implications based on three key localities. J. Geol. Soc. Lond. 161, 711–720.

Udden, J.A., 1907. A Sketch of the Geology of the Chisos Country, Brewster County, Texas. 93. University of Texas Bulletin, Austin, pp. 29–33.

Van Bentum, E.C., Reichart, G.-J., Forster, A., Sinninghe Damasté, J.S., 2012. Latitudinal differences in the amplitude of the OAE-2 carbon isotopic excursion: pCO_2 and paleoproductivity. Biogeosciences 9, 717–731.

Van der Zwaan, G.J., Jorissen, F.J., Stitger, H.C., 1990. The depth dependency of planktonic/benthic foraminiferal ratios: constraints and applications. Mar. Geol. 95, 1–16.

Van Hinsbergen, D.J.J., Kouwenhoven, T.J., Van der Zwaan, G.J., 2005. Paleobathymetry in the backstripping procedure: correction of oxygenation effects on depth estimates. Palaeogeogr. Palaeoclimatol. Palaeoecol. 21, 245–265.

Voigt, S., 2000. Cenomanian–Turonian composite $\delta^{13}C$ for Western and Central Europe: the role of organic and inorganic carbon fluxes. Palaeogeogr. Palaeoclimatol. Palaeoecol. 160, 91–104.

Watkins, D.K., 1985. Biostratigraphy and paleoecology of calcareous nannofossils in the Greenhorn marine cycle. In: Pratt, L.M., Kauffman, E.G., Zelt, F.B. (Eds.), Fine-grained deposits and biofacies of the Cretaceous Western Interior Seaway: evidence of cyclic sedimentary processes. SEPM Mid-year Annual Meeting, Field Trip No. 4, pp. 151–156.

Watkins, D.K., 1986. Calcareous nannofossil paleoceanography of the Cretaceous Greenhorn Sea. Geol. Soc. Am. Bull. 97, 1239–1249.

Watkins, D.K., Bergen, J.A., 2003. Late Albian adaptive radiation in the calcareous nannofossil genus *Eiffellithus*. Micropaleontology 49, 231–252.

Watkins, D.K., Cooper, M.J., Wilson, P.A., 2005. Calcareous nannoplankton response to late Albian oceanic anoxic event in the western North Atlantic. Paleoceanography 20, PA2010. http://dx.doi.org/10.1029/2004PA001097.

West, O.L.O., Leckie, R.M., Schmidt, M., 1998. Paleoceanography of the southwestern Western Interior Sea during the time of the Cenomanian–Turonian boundary (Late Cretaceous). In: Dean, W., Arthur, M.A. (Eds.), Stratigraphy and Paleoenvironments of the Western Interior Seaway, USA. SEPM Concepts in Sedimentology and Paleontology. 6, pp. 79–99.

Williams, J.R., Bralower, T.J., 1995. Nannofossil assemblages, fine fraction stable isotopes, and the paleoceanography of the Valanginian–Barremian (Early Cretaceous) North Sea Basin. Paleoceanography 10, 815–839.

Please cite this article as: Lowery, C.M., et al., Foraminiferal and nannofossil paleoecology and paleoceanography of the Cenomanian–Turonian Eagle Ford Shale of southern Texas, Palaeogeogr. Palaeoclimatol. Palaeoecol. (2014), http://dx.doi.org/10.1016/j.palaeo.2014.07.025